Applied Mathematical Modelling 37 (2013) 4517–4537

Contents lists available at SciVerse ScienceDirect

Applied Mathematical Modelling

journal homepage: www.elsevier.com/locate/apm

Three-dimensional analyses of stress singularities at the vertex of a piezoelectric wedge

C.S. Huang *, C.N. Hu

Department of Civil Engineering, National Chiao Tung University, 1001 Ta-Hsueh Rd., Hsinchu 30050, Taiwan

ARTICLE INFO

Article history:
Received 30 October 2011
Received in revised form 15 August 2012
Accepted 10 September 2012
Available online 21 September 2012

Keywords:
Electroelastic singularities
Piezoelectric wedge
Three-dimensional analysis
Asymptotic solution

ABSTRACT

The electroelastic singularities at the vertex of a rectilinearly polarized piezoelectric wedge are investigated using three-dimensional piezoelasticity theory. An eigenfunction expansion approach is combined with a power series solution technique to find the asymptotic solutions at the vertex of the wedge by directly solving the three-dimensional equilibrium and Maxwell's equations in terms of the displacement components and electric potential. This study is the first to address the problems in which the polarization direction of the piezoelectric material is not necessarily either parallel to the normal of the mid-plane of wedge or in the mid-plane. The correctness of the proposed solution is verified by convergence studies and comparison with the published results that are based on generalized plan strain assumption. The solution is further employed to study comprehensively the effect of the direction of polarization on the electroelastic singularities of wedges that contain a single material (PZT-5H), bounded piezo/isotropic elastic materials (PZT-5H/Si), or piezo/piezo materials (PZT-5H/PZT-4).

1. Introduction

Piezoelectric material is a widely used, smart or intelligent material, because of the intrinsic effects of coupling between electric fields and mechanical deformation. Piezoelectric materials have been extensively applied in actuators, resonators, oscillators, conductors and sensors. The most interesting feature of piezoelectric materials is that they can serve not only as actuators, providing driving signals, but also as sensors for smart structures. In the practical applications, electroelastic singularities are commonly observed at a sharp corner or because of discontinuity in material properties. Accordingly, either local mechanical failure or dielectric failure can occur at a sharp corner. Understanding of the electroelastic singularity behaviors of piezoelectric wedges is essential to optimize the design of piezoelectric devices and further advance smart material technology.

Since Williams [1,2] pioneered the investigation of the stress singularities at a sharp corner of a thin plate under extension or bending with various boundary conditions along the intersecting edges, numerous studies of geometrically-induced stress singularities in isotropic elastic wedges have been conducted. These are based on plane elasticity theory [3–5], three-dimensional elasticity theory [6,7], classical plate theory [8–10], first-order shear deformation plate theory [11–13], third-order plate theory [14], and higher-order plate theory [15]. Nevertheless, much less research has been done on the geometrically-induced electroelastic singularities at the vertex of a piezoelectric wedge.

A few studies of the geometrically-induced electroelastic singularities at the vertex of a piezoelectric wedge (Fig. 1) are based on the assumption that all physical quantities under consideration depend on the planar coordinates. Based on the

* Corresponding author.
E-mail address: cshuang@mail.nctu.edu.tw (C.S. Huang).

0307-904X/$ - see front matter © 2012 Elsevier Inc. All rights reserved.
http://dx.doi.org/10.1016/j.apm.2012.09.021

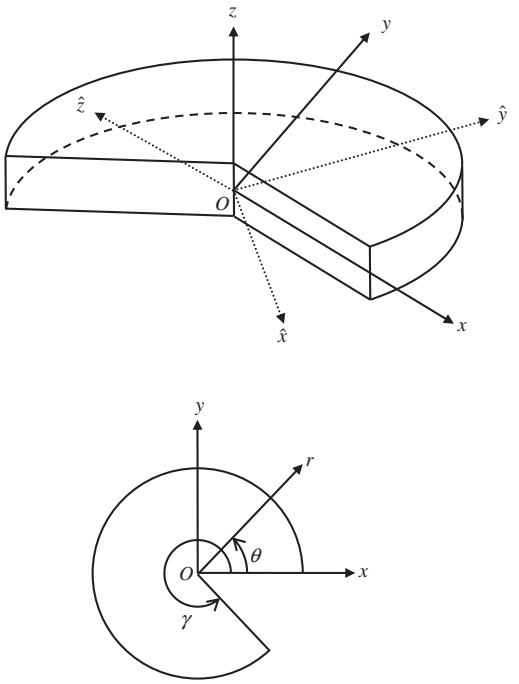

Fig. 1. Coordinate systems for a wedge.

plane strain assumption (ε_{zz},ε_{zy}, ε_{zx}, and E_z, which are defined in Section 2, equal zero), Xu and Rajapakse [16] extended Lekhnitskii's complex potential functions for in-plane stresses and electric displacement components to examine the electroelastic singularities at the vertex of a piezoelectric wedge that has a direction of polarization on the x–y plane (see Fig. 1). Based on an assumption of generalized plane deformation, Chue and Chen [17] presented a decoupled formulation of piezoelectric elasticity and applied it to examine the stress singularities near the apex of a rectilinearly polarized piezoelectric wedge, considering its direction of polarization in the x–y plane or along the z-axis. Hwu and Ikeda [18] proposed an extended Stroh formulation in an (x, y) coordinate system by considering a generalized plane strain and short circuit ($\varepsilon_{zz} = 0$ and $E_z = 0$) and presented numerical results for the electroelastic singularities at the vertices of piezoelectric wedges and multi-material wedges with the directions of polarization in the x–y plane. Because different plane assumptions were made in these three cited papers, they employed different constitutive laws in their solutions. Notably, Xu and Rajapakse [16] treated the piezoelectric material as transversely isotropic material as they began to develop solutions while Chue and Chen [17] and Hwu and Ikeda [18] treated piezoelectric material as generally anisotropic. The solutions of Xu and Rajapakse [16] include only in-plane physical quantities, while those of Chue and Chen [17] and Hwu and Ikeda [18] included in-plane and out-of-plane physical quantities. Following the assumptions in Chue and Chen [17], Chen, Chu and Lee [19] employed the extended Lekhnitskii formulation to determine the eletroelastic singularity behaviors near the apex of a piezoelectric wedge that was polarized in the radial, circular, or axial direction. Chu and Chen [20] applied the Mellin transform to determine anti-plane stress singularities in a bonded bi-material piezoelectric wedge. Neglecting all out-of-plane physical quantities, Shang and Kitamura [21] utilized a modified version of the general solution that was developed by Wang and Zheng [22] and Shang et al. [23] to investigate the stress singularities at the interface edge of a wedge made of two piezoelectric materials with the direction of polarization parallel to the x-axis.

There are several finite element solutions other than the aforementioned analytical solutions in the published literature. Utilizing three-dimensional formulations but assuming all the physical quantities under consideration independent of z (see Fig. 1), Sze et al. [24] combined the eigenfunction expansion technique and a one-dimensional finite element approach to investigate the singularities at the vertex of a piezoelectric wedge. Based on the plane strain assumption, Scherzer and Kuna [25] presented a numerical technique combining asymptotic solutions and a regular finite element approach to solve the piezoelectric field problem of sharp notches at interface configurations. Chen et al. [26] adapted the approach of Sze et al. [24] to investigate in-plane electroelastic singularities at the vertices of piezoelectric wedges and multi-material wedges. Chen and Ping [27,28] further extended the studies in Chen et al. [26] and proposed a super corner-tip element by using the generalized Hellinger–Reissner variational functional.

Although there are some published studies (i.e., [29–32]), which have employed the three-dimensional theory of piezoelectricity to determine the mechanical and electrical fields near a crack tip in a piezoelectric body, no investigation has conducted three-dimensional analyses of geometrically-induced electroelastic singularities at the vertex of a piezoelectric wedge. The main purpose of this paper is to present a three-dimensional asymptotic solution for the electroelastic singularities at the vertex of a piezoelectric wedge without assuming that the direction of polarization of the material is either along

the z-axis or in the x–y plane. An eigenfunction expansion scheme is combined with a power series method to solve the equilibrium and Maxwell's equations in terms of mechanical displacement components and electric potential in a cylindrical coordinate system. The correctness of the proposed solution is ensured by comparison with the published results based on the generalized plane strain assumption. The solution is further employed to examine thoroughly the effects of polarization direction, wedge angle, and boundary conditions on the electroelastic singularities of wedges that comprise a single material (PZT-5H), bounded piezo/isotropic elastic materials (PZT-5H/Si), or piezo/piezo materials (PZT-5H/PZT-4). The numerical results concerning the order of the singularity are expressed in graphic form, and are shown herein for the first time.

2. Basic formulation

Consider a rectilinearly anisotropic piezoelectric wedge that is polarized in the $\hat{z}$ direction, as presented in Fig. 1. The constitutive equations of the piezoelectric material are expressed in the material coordinate system $(\hat{x},\hat{y},\hat{z})$, as

$$\{\hat{\sigma}\} = [\hat{c}]\{\hat{\varepsilon}\} - [\hat{e}]^T\{\hat{E}\}, \tag{1a}$$

$$\{\hat{D}\} = [\hat{e}]\{\hat{\varepsilon}\} + [\hat{\eta}]\{\hat{E}\}, \tag{1b}$$

where $\{\hat{\sigma}\} = \{\,\sigma_{\hat{x}\hat{x}} \quad \sigma_{\hat{y}\hat{y}} \quad \sigma_{\hat{z}\hat{z}} \quad \sigma_{\hat{y}\hat{z}} \quad \sigma_{\hat{z}\hat{x}} \quad \sigma_{\hat{x}\hat{y}}\,\}^T$ is the stress vector;

$\{\hat{\varepsilon}\} = \{\,\varepsilon_{\hat{x}\hat{x}} \quad \varepsilon_{\hat{y}\hat{y}} \quad \varepsilon_{\hat{z}\hat{z}} \quad 2\varepsilon_{\hat{y}\hat{z}} \quad 2\varepsilon_{\hat{z}\hat{x}} \quad 2\varepsilon_{\hat{x}\hat{y}}\,\}^T$ is the strain vector; $\{\hat{D}\} = \{\,D_{\hat{x}} \quad D_{\hat{y}} \quad D_{\hat{z}}\,\}^T$ is the electric displacement vector; $\{\hat{E}\} = \{\,E_{\hat{x}} \quad E_{\hat{y}} \quad E_{\hat{z}}\,\}^T$ is the electric field vector, and $[\hat{c}]$, $[\hat{e}]$ and $[\hat{\eta}]$ are the mechanical elastic constant matrix, the piezoelectric constant matrix and the dielectric constant matrix, respectively.

It is easy to solve for the eletroelastic singularities at the vertex of the wedge in the cylindrical coordinate system (r,θ,z) given in Fig. 1. In the cylindrical coordinate system, the equilibrium and Maxwell's equations in terms of stress components (σ_{ij}) and electric displacements (D_i) without body force and charges are [33]

$$\frac{\partial\sigma_{rr}}{\partial r} + \frac{1}{r}\frac{\partial\sigma_{r\theta}}{\partial\theta} + \frac{\partial\sigma_{rz}}{\partial z} + \frac{(\sigma_{rr}-\sigma_{\theta\theta})}{r} = 0, \tag{2a}$$

$$\frac{\partial\sigma_{r\theta}}{\partial r} + \frac{1}{r}\frac{\partial\sigma_{\theta\theta}}{\partial\theta} + \frac{\partial\sigma_{\theta z}}{\partial z} + 2\frac{\sigma_{r\theta}}{r} = 0, \tag{2b}$$

$$\frac{\partial\sigma_{rz}}{\partial r} + \frac{1}{r}\frac{\partial\sigma_{\theta z}}{\partial\theta} + \frac{\partial\sigma_{zz}}{\partial z} + \frac{\sigma_{rz}}{r} = 0, \tag{2c}$$

$$\frac{1}{r}\frac{\partial(rD_r)}{\partial r} + \frac{1}{r}\frac{\partial D_\theta}{\partial\theta} + \frac{\partial D_z}{\partial z} = 0, \tag{2d}$$

The constitutive equations of the piezoelectric material in the cylindrical coordinate system are

$$\{\sigma\} = [c]\{\varepsilon\} - [e]^T\{E\}, \tag{3a}$$

$$\{D\} = [e]\{\varepsilon\} + [\eta]\{E\}, \tag{3b}$$

where $\{\sigma\} = \{\,\sigma_{rr} \quad \sigma_{\theta\theta} \quad \sigma_{zz} \quad \sigma_{\theta z} \quad \sigma_{zr} \quad \sigma_{r\theta}\,\}^T$, $\{\varepsilon\} = \{\,\varepsilon_{rr} \quad \varepsilon_{\theta\theta} \quad \varepsilon_{zz} \quad 2\varepsilon_{\theta z} \quad 2\varepsilon_{zr} \quad 2\varepsilon_{r\theta}\,\}^T$, $\{D\} = \{\,D_r \quad D_\theta \quad D_z\,\}^T$, $\{E\} = \{\,E_r \quad E_\theta \quad E_z\,\}^T$,

$$[c] = \begin{bmatrix} c_{11} & c_{12} & c_{13} & c_{14} & c_{15} & c_{16} \\ c_{12} & c_{22} & c_{23} & c_{24} & c_{25} & c_{26} \\ c_{13} & c_{23} & c_{33} & c_{34} & c_{35} & c_{36} \\ c_{14} & c_{24} & c_{34} & c_{44} & c_{45} & c_{46} \\ c_{15} & c_{25} & c_{35} & c_{45} & c_{55} & c_{56} \\ c_{16} & c_{26} & c_{36} & c_{46} & c_{56} & c_{66} \end{bmatrix}, \quad [e] = \begin{bmatrix} e_{11} & e_{12} & e_{13} & e_{14} & e_{15} & e_{16} \\ e_{21} & e_{22} & e_{23} & e_{24} & e_{25} & e_{26} \\ e_{31} & e_{32} & e_{33} & e_{34} & e_{35} & e_{36} \end{bmatrix},$$

$$[\eta] = \begin{bmatrix} \eta_{11} & \eta_{12} & \eta_{13} \\ \eta_{12} & \eta_{22} & \eta_{23} \\ \eta_{13} & \eta_{23} & \eta_{33} \end{bmatrix}. \tag{4}$$

The components of $[c]$, $[e]$ and $[\eta]$ are related to the components of $[\hat{c}]$, $[\hat{e}]$ and $[\hat{\eta}]$, respectively; and are functions of θ and depend on the direction cosines between $(\hat{x},\hat{y},\hat{z})$ and (x,y,z). These relations are given in Appendix I.

Substituting strain–displacement relations and electric field–potential relations into Eqs. (3) and (4) enables the stress components and electric displacements to be expressed in terms of mechanical displacement components (u_r,u_θ and u_z)

and electric potential (ϕ), given in Appendix II. Substituting those expressions into Eqs. (2) yields the governing equations in terms of mechanical displacement components and electric potential as

$$
\begin{aligned}
&[c_{11}\frac{\partial^2}{\partial r^2}+c_{55}\frac{\partial^2}{\partial z^2}+(c_{11}+\frac{\partial c_{16}}{\partial\theta})\frac{\partial}{r\partial r}+(c_{15}+\frac{\partial c_{56}}{\partial\theta})\frac{\partial}{r\partial z}+\frac{\partial c_{66}}{\partial\theta}\frac{\partial}{r^2\partial\theta}+2c_{16}\frac{\partial^2}{r\partial r\partial\theta}+2c_{56}\frac{\partial^2}{r\partial\theta\partial z}+2c_{15}\frac{\partial^2}{\partial r\partial z}\\
&+(-c_{22}+\frac{\partial c_{26}}{\partial\theta}+c_{66}\frac{\partial^2}{\partial\theta^2})\frac{1}{r^2}]u_r+[c_{16}\frac{\partial^2}{\partial r^2}+c_{45}\frac{\partial^2}{\partial z^2}+(-c_{26}+\frac{\partial c_{66}}{\partial\theta})\frac{\partial}{r\partial r}+(c_{14}-c_{24}-c_{56}+\frac{\partial c_{46}}{\partial\theta})\frac{\partial}{r\partial z}\\
&+(-c_{22}-c_{66}+\frac{\partial c_{26}}{\partial\theta})\frac{\partial}{r^2\partial\theta}+(c_{12}+c_{66})\frac{\partial^2}{r\partial r\partial\theta}+(c_{25}+c_{46})\frac{\partial^2}{r\partial\theta\partial z}+(c_{14}+c_{56})\frac{\partial^2}{\partial r\partial z}+(c_{26}-\frac{\partial c_{66}}{\partial\theta}+c_{26}\frac{\partial^2}{\partial\theta^2})\frac{1}{r^2}]u_\theta\\
&+[c_{15}\frac{\partial^2}{\partial r^2}+c_{35}\frac{\partial^2}{\partial z^2}+(c_{15}-c_{25}+\frac{\partial c_{56}}{\partial\theta})\frac{\partial}{r\partial r}+(c_{13}-c_{23}+\frac{\partial c_{36}}{\partial\theta})\frac{\partial}{r\partial z}+(-c_{24}+\frac{\partial c_{46}}{\partial\theta})\frac{\partial}{r^2\partial\theta}+(c_{14}+c_{56})\frac{\partial^2}{r\partial r\partial\theta}\\
&+(c_{36}+c_{45})\frac{\partial^2}{r\partial\theta\partial z}+(c_{13}+c_{55})\frac{\partial^2}{\partial r\partial z}+c_{46}\frac{\partial^2}{r^2\partial\theta^2}]u_z+[e_{11}\frac{\partial^2}{\partial r^2}+e_{35}\frac{\partial^2}{\partial z^2}+(e_{11}-e_{12}+\frac{\partial e_{16}}{\partial\theta})\frac{\partial}{r\partial r}\\
&+(e_{31}-e_{32}+\frac{\partial e_{36}}{\partial\theta})\frac{\partial}{r\partial z}+(-e_{22}+\frac{\partial e_{26}}{\partial\theta})\frac{\partial}{r^2\partial\theta}+(e_{16}+e_{21})\frac{\partial^2}{r\partial r\partial\theta}+(e_{25}+e_{36})\frac{\partial^2}{r\partial\theta\partial z}+(e_{31}+e_{15})\frac{\partial^2}{\partial r\partial z}+e_{26}\frac{\partial^2}{r^2\partial\theta^2}]\phi=0
\end{aligned}
\tag{5a}
$$

$$
\begin{aligned}
&[c_{16}\frac{\partial^2}{\partial r^2}+c_{45}\frac{\partial^2}{\partial z^2}+(2c_{16}+c_{26}+\frac{\partial c_{12}}{\partial\theta})\frac{\partial}{r\partial r}+(2c_{56}+c_{24}+\frac{\partial c_{25}}{\partial\theta})\frac{\partial}{r\partial z}+(c_{22}+c_{66}+\frac{\partial c_{26}}{\partial\theta})\frac{\partial}{r^2\partial\theta}+(c_{12}+c_{66})\frac{\partial^2}{r\partial r\partial\theta}\\
&+(c_{25}+c_{46})\frac{\partial^2}{r\partial\theta\partial z}+(c_{56}+c_{14})\frac{\partial^2}{\partial r\partial z}+(c_{26}+\frac{\partial c_{22}}{\partial\theta}+c_{26}\frac{\partial^2}{\partial\theta^2})\frac{1}{r^2}]u_r+[c_{66}\frac{\partial^2}{\partial r^2}+c_{44}\frac{\partial^2}{\partial z^2}+(c_{66}+\frac{\partial c_{26}}{\partial\theta})\frac{\partial}{r\partial r}\\
&+(c_{46}+\frac{\partial c_{24}}{\partial\theta})\frac{\partial}{r\partial z}+(\frac{\partial c_{22}}{\partial\theta})\frac{\partial}{r^2\partial\theta}+2c_{26}\frac{\partial^2}{r\partial r\partial\theta}+2c_{24}\frac{\partial^2}{r\partial\theta\partial z}+2c_{46}\frac{\partial^2}{\partial r\partial z}+(-c_{66}-\frac{\partial c_{26}}{\partial\theta}+c_{22}\frac{\partial^2}{\partial\theta^2})\frac{1}{r^2}]u_\theta\\
&+[c_{56}\frac{\partial^2}{\partial r^2}+c_{34}\frac{\partial^2}{\partial z^2}+(2c_{56}+\frac{\partial c_{25}}{\partial\theta})\frac{\partial}{r\partial r}+(2c_{36}+\frac{\partial c_{23}}{\partial\theta})\frac{\partial}{r\partial z}+(c_{46}+\frac{\partial c_{24}}{\partial\theta})\frac{\partial}{r^2\partial\theta}+(c_{25}+c_{46})\frac{\partial^2}{r\partial r\partial\theta}\\
&+(c_{23}+c_{44})\frac{\partial^2}{r\partial\theta\partial z}+(c_{36}+c_{45})\frac{\partial^2}{\partial r\partial z}+c_{24}\frac{\partial^2}{r^2\partial\theta^2}]u_z+[e_{16}\frac{\partial^2}{\partial r^2}+e_{34}\frac{\partial^2}{\partial z^2}+(2e_{16}+\frac{\partial e_{12}}{\partial\theta})\frac{\partial}{r\partial r}+(2e_{36}+\frac{\partial e_{32}}{\partial\theta})\frac{\partial}{r\partial z}\\
&+(e_{26}+\frac{\partial e_{22}}{\partial\theta})\frac{\partial}{r^2\partial\theta}+(e_{12}+e_{26})\frac{\partial^2}{r\partial r\partial\theta}+(e_{24}+e_{32})\frac{\partial^2}{r\partial\theta\partial z}+(e_{36}+e_{14})\frac{\partial^2}{\partial r\partial z}+e_{22}\frac{\partial^2}{r^2\partial\theta^2}]\phi=0,
\end{aligned}
\tag{5b}
$$

$$
\begin{aligned}
&[c_{15}\frac{\partial^2}{\partial r^2}+c_{35}\frac{\partial^2}{\partial z^2}+(c_{15}+c_{25}+\frac{\partial c_{14}}{\partial\theta})\frac{\partial}{r\partial r}+(c_{23}+c_{55}+\frac{\partial c_{45}}{\partial\theta})\frac{\partial}{r\partial z}+(c_{24}+\frac{\partial c_{46}}{\partial\theta})\frac{\partial}{r^2\partial\theta}+(c_{14}+c_{56})\frac{\partial^2}{r\partial r\partial\theta}\\
&+(c_{45}+c_{36})\frac{\partial^2}{r\partial\theta\partial z}+(c_{55}+c_{13})\frac{\partial^2}{\partial r\partial z}+(\frac{\partial c_{24}}{\partial\theta}+c_{46}\frac{\partial^2}{\partial\theta^2})\frac{1}{r^2}]u_r+[c_{56}\frac{\partial^2}{\partial r^2}+c_{34}\frac{\partial^2}{\partial z^2}+(\frac{\partial c_{46}}{\partial\theta})\frac{\partial}{r\partial r}\\
&+(c_{45}-c_{36}+\frac{\partial c_{44}}{\partial\theta})\frac{\partial}{r\partial z}+(-c_{46}+\frac{\partial c_{24}}{\partial\theta})\frac{\partial}{r^2\partial\theta}+(c_{25}+c_{46})\frac{\partial^2}{r\partial r\partial\theta}+(c_{44}+c_{23})\frac{\partial^2}{r\partial\theta\partial z}+(c_{45}+c_{36})\frac{\partial^2}{\partial r\partial z}\\
&+(-\frac{\partial c_{46}}{\partial\theta}+c_{24}\frac{\partial^2}{\partial\theta^2})\frac{1}{r^2}]u_\theta+[c_{55}\frac{\partial^2}{\partial r^2}+c_{33}\frac{\partial^2}{\partial z^2}+(c_{55}+\frac{\partial c_{45}}{\partial\theta})\frac{\partial}{r\partial r}+(c_{35}+\frac{\partial c_{34}}{\partial\theta})\frac{\partial}{r\partial z}+(\frac{\partial c_{44}}{\partial\theta})\frac{\partial}{r^2\partial\theta}+2c_{45}\frac{\partial^2}{r\partial r\partial\theta}\\
&+2c_{34}\frac{\partial^2}{r\partial\theta\partial z}+2c_{35}\frac{\partial^2}{\partial r\partial z}+c_{44}\frac{\partial^2}{r^2\partial\theta^2}]u_z+[e_{15}\frac{\partial^2}{\partial r^2}+e_{33}\frac{\partial^2}{\partial z^2}+(e_{15}+\frac{\partial e_{14}}{\partial\theta})\frac{\partial}{r\partial r}+(e_{35}+\frac{\partial e_{34}}{\partial\theta})\frac{\partial}{r\partial z}+(\frac{\partial e_{24}}{\partial\theta})\frac{\partial}{r^2\partial\theta}\\
&+(e_{25}+e_{14})\frac{\partial^2}{r\partial r\partial\theta}+(e_{34}+e_{23})\frac{\partial^2}{r\partial\theta\partial z}+(e_{35}+e_{13})\frac{\partial^2}{\partial r\partial z}+e_{24}\frac{\partial^2}{r^2\partial\theta^2}]\phi=0,
\end{aligned}
\tag{5c}
$$

$$
\begin{aligned}
&[e_{11}\frac{\partial^2}{\partial r^2}+e_{35}\frac{\partial^2}{\partial z^2}+(e_{11}+e_{12}+\frac{\partial e_{21}}{\partial\theta})\frac{\partial}{r\partial r}+(e_{15}+e_{32}+\frac{\partial e_{25}}{\partial\theta})\frac{\partial}{r\partial z}+(e_{22}+\frac{\partial e_{26}}{\partial\theta})\frac{\partial}{r^2\partial\theta}+(e_{16}+e_{21})\frac{\partial^2}{r\partial r\partial\theta}\\
&+(e_{25}+e_{36})\frac{\partial^2}{r\partial\theta\partial z}+(e_{15}+e_{31})\frac{\partial^2}{\partial r\partial z}+(\frac{\partial e_{22}}{\partial\theta}+e_{26}\frac{\partial^2}{\partial\theta^2})\frac{1}{r^2}]u_r+[e_{16}\frac{\partial^2}{\partial r^2}+e_{34}\frac{\partial^2}{\partial z^2}+(\frac{\partial e_{26}}{\partial\theta})\frac{\partial}{r\partial r}+(e_{14}-e_{36}+\frac{\partial e_{24}}{\partial\theta})\frac{\partial}{r\partial z}\\
&+(-e_{26}+\frac{\partial e_{22}}{\partial\theta})\frac{\partial}{r^2\partial\theta}+(e_{12}+e_{26})\frac{\partial^2}{r\partial r\partial\theta}+(e_{24}+e_{32})\frac{\partial^2}{r\partial\theta\partial z}+(e_{14}+e_{36})\frac{\partial^2}{\partial r\partial z}+(-\frac{\partial e_{26}}{\partial\theta}+e_{22}\frac{\partial^2}{\partial\theta^2})\frac{1}{r^2}]u_\theta\\
&+[e_{15}\frac{\partial^2}{\partial r^2}+e_{33}\frac{\partial^2}{\partial z^2}+(e_{15}+\frac{\partial e_{25}}{\partial\theta})\frac{\partial}{r\partial r}+(e_{13}+\frac{\partial e_{23}}{\partial\theta})\frac{\partial}{r\partial z}+(\frac{\partial e_{24}}{\partial\theta})\frac{\partial}{r^2\partial\theta}+(e_{14}+e_{25})\frac{\partial^2}{r\partial r\partial\theta}+(e_{23}+e_{34})\frac{\partial^2}{r\partial\theta\partial z}\\
&+(e_{13}+e_{35})\frac{\partial^2}{\partial r\partial z}+e_{24}\frac{\partial^2}{r^2\partial\theta^2}]u_z-[\eta_{11}\frac{\partial^2}{\partial r^2}+\eta_{33}\frac{\partial^2}{\partial z^2}+(\eta_{11}+\frac{\partial\eta_{12}}{\partial\theta})\frac{\partial}{r\partial r}+(\frac{\partial\eta_{22}}{\partial\theta})\frac{\partial}{r^2\partial\theta}+(\eta_{13}+\frac{\partial\eta_{23}}{\partial\theta})\frac{\partial}{r\partial z}\\
&+2\eta_{12}\frac{\partial^2}{r\partial r\partial\theta}+2\eta_{23}\frac{\partial^2}{r\partial\theta\partial z}+2\eta_{13}\frac{\partial^2}{\partial r\partial z}+\eta_{22}\frac{\partial^2}{r^2\partial\theta^2}]\phi=0.
\end{aligned}
\tag{5d}
$$

3. Construction of asymptotic solution

To determine the asymptotic solution of Eqs. (5) as r approaches zero, the mechanical displacement components and electric potential in the double series can be conveniently expanded as follows;

$$u_r(r,\theta,z)=\sum_{m=0}^{\infty}\sum_{n=0}^{\infty}r^{\lambda_m+n}\hat{U}_n^{(m)}(\theta,z), \tag{6a}$$

$$u_\theta(r,\theta,z)=\sum_{m=0}^{\infty}\sum_{n=0}^{\infty}r^{\lambda_m+n}\hat{V}_n^{(m)}(\theta,z), \tag{6b}$$

$$u_z(r,\theta,z)=\sum_{m=0}^{\infty}\sum_{n=0}^{\infty}r^{\lambda_m+n}\hat{W}_n^{(m)}(\theta,z), \tag{6c}$$

$$\phi(r,\theta,z)=\sum_{m=0}^{\infty}\sum_{n=0}^{\infty}r^{\lambda_m+n}\hat{\Phi}_n^{(m)}(\theta,z), \tag{6d}$$

where the characteristic values λ_m are assumed to be constants and can be complex numbers. The real part of λ_m has to be positive to satisfy the regularity conditions for mechanical displacement components and electric potential at $r=0$ (such as finite displacement and electric potential at $r=0$).

Substituting Eqs. (6) into Eqs. (5) and carefully arranging the resulting equations yields,

$$\begin{aligned}
&\sum_{m=0}^{\infty}\sum_{n=0}^{\infty}r^{\lambda_m+n-2}[c_{11}(\lambda_m+n)(\lambda_m+n-1)\hat{U}_n^{(m)}+(c_{11}+\frac{\partial c_{16}}{\partial\theta})(\lambda_m+n)\hat{U}_n^{(m)}+\frac{\partial c_{66}}{\partial\theta}\frac{\partial\hat{U}_n^{(m)}}{\partial\theta}+2c_{16}(\lambda_m+n)\frac{\partial\hat{U}_n^{(m)}}{\partial\theta}\\
&\quad+(-c_{22}+\frac{\partial c_{26}}{\partial\theta}+c_{66}\frac{\partial^2}{\partial\theta^2})\hat{U}_n^{(m)}+c_{16}(\lambda_m+n)(\lambda_m+n-1)\hat{V}_n^{(m)}+(-c_{26}+\frac{\partial c_{66}}{\partial\theta})(\lambda_m+n)\hat{V}_n^{(m)}+(-c_{22}-c_{66}+\frac{\partial c_{26}}{\partial\theta})\frac{\partial\hat{V}_n^{(m)}}{\partial\theta}\\
&\quad+(c_{12}+c_{66})(\lambda_m+n)\frac{\partial\hat{V}_n^{(m)}}{\partial\theta}+(c_{26}-\frac{\partial c_{66}}{\partial\theta}+c_{26}\frac{\partial^2}{\partial\theta^2})\hat{V}_n^{(m)}+c_{15}(\lambda_m+n)(\lambda_m+n-1)\hat{W}_n^{(m)}\\
&\quad+(c_{15}-c_{25}+\frac{\partial c_{56}}{\partial\theta})(\lambda_m+n)\hat{W}_n^{(m)}+(-c_{24}+\frac{\partial c_{46}}{\partial\theta})\frac{\partial\hat{W}_n^{(m)}}{\partial\theta}+(c_{14}+c_{56})(\lambda_m+n)\frac{\partial\hat{W}_n^{(m)}}{\partial\theta}+c_{46}\frac{\partial^2\hat{W}_n^{(m)}}{\partial\theta^2}\\
&\quad+e_{11}(\lambda_m+n)(\lambda_m+n-1)\hat{\Phi}_n^{(m)}+(e_{11}-e_{12}+\frac{\partial e_{16}}{\partial\theta})(\lambda_m+n)\hat{\Phi}_n^{(m)}+(-e_{22}+\frac{\partial e_{26}}{\partial\theta})\frac{\partial\hat{\Phi}_n^{(m)}}{\partial\theta}+(e_{16}+e_{21})(\lambda_m+n)\frac{\partial\hat{\Phi}_n^{(m)}}{\partial\theta}\\
&\quad+e_{26}\frac{\partial^2\hat{\Phi}_n^{(m)}}{\partial\theta^2}]+r^{\lambda_m+n-1}[(c_{15}+\frac{\partial c_{56}}{\partial\theta})\frac{\partial\hat{U}_n^{(m)}}{\partial z}+2c_{56}\frac{\partial^2\hat{U}_n^{(m)}}{\partial\theta\partial z}+2c_{15}(\lambda_m+n)\frac{\partial\hat{U}_n^{(m)}}{\partial z}+(c_{14}-c_{24}-c_{56}+\frac{\partial c_{46}}{\partial\theta})\frac{\partial\hat{V}_n^{(m)}}{\partial z}\\
&\quad+(c_{25}+c_{46})\frac{\partial^2\hat{V}_n^{(m)}}{\partial\theta\partial z}+(c_{14}+c_{56})(\lambda_m+n)\frac{\partial\hat{V}_n^{(m)}}{\partial z}+(c_{36}+c_{45})\frac{\partial^2\hat{W}_n^{(m)}}{\partial\theta\partial z}+(c_{13}-c_{23}+\frac{\partial c_{36}}{\partial\theta})\frac{\partial\hat{W}_n^{(m)}}{\partial z}\\
&\quad+(c_{13}+c_{55})(\lambda_m+n)\frac{\partial\hat{W}_n^{(m)}}{\partial z}+(e_{31}-e_{32}+\frac{\partial e_{36}}{\partial\theta})\frac{\partial\hat{\Phi}_n^{(m)}}{\partial z}+(e_{25}+e_{36})\frac{\partial^2\hat{\Phi}_n^{(m)}}{\partial\theta\partial z}+(e_{31}+e_{15})(\lambda_m+n)\frac{\partial\hat{\Phi}_n^{(m)}}{\partial z}]\\
&\quad+r^{\lambda_m+n}(c_{55}\frac{\partial^2\hat{U}_n^{(m)}}{\partial z^2}+c_{45}\frac{\partial^2\hat{V}_n^{(m)}}{\partial z^2}+c_{35}\frac{\partial^2\hat{W}_n^{(m)}}{\partial z^2}+e_{35}\frac{\partial^2\hat{\Phi}_n^{(m)}}{\partial z^2})=0,
\end{aligned} \tag{7a}$$

$$\begin{aligned}
&\sum_{m=0}^{\infty}\sum_{n=0}^{\infty}r^{\lambda_m+n-2}[c_{16}(\lambda_m+n)(\lambda_m+n-1)\hat{U}_n^{(m)}+(2c_{16}+c_{26}+\frac{\partial c_{12}}{\partial\theta})(\lambda_m+n)\hat{U}_n^{(m)}+(c_{22}+c_{66}+\frac{\partial c_{26}}{\partial\theta})\frac{\partial\hat{U}_n^{(m)}}{\partial\theta}\\
&\quad+(c_{12}+c_{66})(\lambda_m+n)\frac{\partial\hat{U}_n^{(m)}}{\partial\theta}+(c_{26}+\frac{\partial c_{22}}{\partial\theta}+c_{26}\frac{\partial^2}{\partial\theta^2})\hat{U}_n^{(m)}+c_{66}(\lambda_m+n)(\lambda_m+n-1)\hat{V}_n^{(m)}+(\frac{\partial c_{22}}{\partial\theta})\frac{\partial\hat{V}_n^{(m)}}{\partial\theta}\\
&\quad+(c_{66}+\frac{\partial c_{26}}{\partial\theta})(\lambda_m+n)\hat{V}_n^{(m)}+2c_{26}(\lambda_m+n)\frac{\partial\hat{V}_n^{(m)}}{\partial\theta}+(-c_{66}-\frac{\partial c_{26}}{\partial\theta}+c_{22}\frac{\partial^2}{\partial\theta^2})\hat{V}_n^{(m)}+c_{56}(\lambda_m+n)(\lambda_m+n-1)\hat{W}_n^{(m)}\\
&\quad+(2c_{56}+\frac{\partial c_{25}}{\partial\theta})(\lambda_m+n)\hat{W}_n^{(m)}+(c_{46}+\frac{\partial c_{24}}{\partial\theta})\frac{\partial\hat{W}_n^{(m)}}{\partial\theta}+(c_{25}+c_{46})(\lambda_m+n)\frac{\partial\hat{W}_n^{(m)}}{\partial\theta}+c_{24}\frac{\partial^2\hat{W}_n^{(m)}}{\partial\theta^2}+e_{16}(\lambda_m+n)(\lambda_m+n-1)\hat{\Phi}_n^{(m)}\\
&\quad+(2e_{16}+\frac{\partial e_{12}}{\partial\theta})(\lambda_m+n)\hat{\Phi}_n^{(m)}+(e_{26}+\frac{\partial e_{22}}{\partial\theta})\frac{\partial\hat{\Phi}_n^{(m)}}{\partial\theta}+(e_{12}+e_{26})(\lambda_m+n)\frac{\partial\hat{\Phi}_n^{(m)}}{\partial\theta}+e_{22}\frac{\partial^2\hat{\Phi}_n^{(m)}}{\partial\theta^2}]\\
&\quad+r^{\lambda_m+n-1}[(2c_{56}+c_{24}+\frac{\partial c_{25}}{\partial\theta})\frac{\partial\hat{U}_n^{(m)}}{\partial z}+(c_{25}+c_{46})\frac{\partial^2\hat{U}_n^{(m)}}{\partial\theta\partial z}+(c_{56}+c_{14})(\lambda_m+n)\frac{\partial\hat{U}_n^{(m)}}{\partial z}+(c_{46}+\frac{\partial c_{24}}{\partial\theta})\frac{\partial\hat{V}_n^{(m)}}{\partial z}\\
&\quad+2c_{24}\frac{\partial^2\hat{V}_n^{(m)}}{\partial\theta\partial z}+2c_{46}(\lambda_m+n)\frac{\partial\hat{V}_n^{(m)}}{\partial z}+(2c_{36}+\frac{\partial c_{23}}{\partial\theta})\frac{\partial\hat{W}_n^{(m)}}{\partial z}+(c_{23}+c_{44})\frac{\partial^2\hat{W}_n^{(m)}}{\partial\theta\partial z}+(c_{36}+c_{45})(\lambda_m+n)\frac{\partial\hat{W}_n^{(m)}}{\partial z}\\
&\quad+(2e_{36}+\frac{\partial e_{32}}{\partial\theta})\frac{\partial\hat{\Phi}_n^{(m)}}{\partial z}+(e_{24}+e_{32})\frac{\partial^2\hat{\Phi}_n^{(m)}}{\partial\theta\partial z}+(e_{36}+e_{14})(\lambda_m+n)\frac{\partial\hat{\Phi}_n^{(m)}}{\partial z}]+r^{\lambda_m+n}(c_{45}\frac{\partial^2\hat{U}_n^{(m)}}{\partial z^2}+c_{44}\frac{\partial^2\hat{V}_n^{(m)}}{\partial z^2}\\
&\quad+c_{34}\frac{\partial^2\hat{W}_n^{(m)}}{\partial z^2}+e_{34}\frac{\partial^2\hat{\Phi}_n^{(m)}}{\partial z^2})=0,
\end{aligned} \tag{7b}$$

$$\sum_{m=0}^{\infty}\sum_{n=0}^{\infty} r^{\lambda_m+n-2}[c_{15}(\lambda_m+n)(\lambda_m+n-1)\hat{U}_n^{(m)} + (c_{15}+c_{25}+\frac{\partial c_{14}}{\partial\theta})(\lambda_m+n)\hat{U}_n^{(m)} + (c_{24}+\frac{\partial c_{46}}{\partial\theta})\frac{\partial\hat{U}_n^{(m)}}{\partial\theta}$$
$$+ (c_{14}+c_{56})(\lambda_m+n)\frac{\partial\hat{U}_n^{(m)}}{\partial\theta} + (\frac{\partial c_{24}}{\partial\theta}+c_{46}\frac{\partial^2}{\partial\theta^2})\hat{U}_n^{(m)} + c_{56}(\lambda_m+n)(\lambda_m+n-1)\hat{V}_n^{(m)} + (\frac{\partial c_{46}}{\partial\theta})(\lambda_m+n)\hat{V}_n^{(m)}$$
$$+ (-c_{46}+\frac{\partial c_{24}}{\partial\theta})\frac{\partial\hat{V}_n^{(m)}}{\partial\theta} + (c_{25}+c_{46})(\lambda_m+n)\frac{\partial\hat{V}_n^{(m)}}{\partial\theta} + (-\frac{\partial c_{46}}{\partial\theta}+c_{24}\frac{\partial^2}{\partial\theta^2})\hat{V}_n^{(m)} + c_{55}(\lambda_m+n)(\lambda_m+n-1)\hat{W}_n^{(m)}$$
$$+ (c_{55}+\frac{\partial c_{45}}{\partial\theta})(\lambda_m+n)\hat{W}_n^{(m)} + (\frac{\partial c_{44}}{\partial\theta})\frac{\partial\hat{W}_n^{(m)}}{\partial\theta} + 2c_{45}(\lambda_m+n)\frac{\partial\hat{W}_n^{(m)}}{\partial\theta} + c_{44}\frac{\partial^2\hat{W}_n^{(m)}}{\partial\theta^2} + e_{15}(\lambda_m+n)(\lambda_m+n-1)\hat{\Phi}_n^{(m)}$$
$$+ (e_{15}+\frac{\partial e_{14}}{\partial\theta})(\lambda_m+n)\hat{\Phi}_n^{(m)} + (\frac{\partial e_{24}}{\partial\theta})\frac{\partial\hat{\Phi}_n^{(m)}}{\partial\theta} + (e_{25}+e_{14})(\lambda_m+n)\frac{\partial\hat{\Phi}_n^{(m)}}{\partial\theta} + e_{24}\frac{\partial^2\hat{\Phi}_n^{(m)}}{\partial\theta^2}] + r^{\lambda_m+n-1}[(c_{23}+c_{55}+\frac{\partial c_{45}}{\partial\theta})\frac{\partial\hat{U}_n^{(m)}}{\partial z}$$
$$+ (c_{45}+c_{36})\frac{\partial^2\hat{U}_n^{(m)}}{\partial\theta\partial z} + (c_{55}+c_{13})(\lambda_m+n)\frac{\partial\hat{U}_n^{(m)}}{\partial z} + (c_{45}-c_{36}+\frac{\partial c_{24}}{\partial\theta})\frac{\partial\hat{V}_n^{(m)}}{\partial z} + (c_{44}+c_{23})\frac{\partial^2\hat{V}_n^{(m)}}{\partial\theta\partial z}$$
$$+ (c_{45}+c_{36})(\lambda_m+n)\frac{\partial\hat{V}_n^{(m)}}{\partial z} + (c_{35}+\frac{\partial c_{34}}{\partial\theta})\frac{\partial\hat{W}_n^{(m)}}{\partial z} + 2c_{34}\frac{\partial^2\hat{W}_n^{(m)}}{\partial\theta\partial z} + 2c_{35}(\lambda_m+n)\frac{\partial\hat{W}_n^{(m)}}{\partial z} + (e_{35}+\frac{\partial e_{34}}{\partial\theta})\frac{\partial\hat{\Phi}_n^{(m)}}{\partial z}$$
$$+ (e_{34}+e_{23})\frac{\partial^2\hat{\Phi}_n^{(m)}}{\partial\theta\partial z} + (e_{35}+e_{13})(\lambda_m+n)\frac{\partial\hat{\Phi}_n^{(m)}}{\partial z}] + r^{\lambda_m+n}(c_{35}\frac{\partial^2\hat{U}_n^{(m)}}{\partial z^2} + c_{34}\frac{\partial^2\hat{V}_n^{(m)}}{\partial z^2} + c_{33}\frac{\partial^2\hat{W}_n^{(m)}}{\partial z^2} + e_{33}\frac{\partial^2\hat{\Phi}_n^{(m)}}{\partial z^2}) = 0, \quad (7c)$$

$$\sum_{m=0}^{\infty}\sum_{n=0}^{\infty} r^{\lambda_m+n-2}[e_{11}(\lambda_m+n)(\lambda_m+n-1)\hat{U}_n^{(m)} + (e_{11}+e_{12}+\frac{\partial e_{21}}{\partial\theta})(\lambda_m+n)\hat{U}_n^{(m)} + (e_{22}+\frac{\partial e_{26}}{\partial\theta})\frac{\partial\hat{U}_n^{(m)}}{\partial\theta}$$
$$+ (e_{16}+e_{21})(\lambda_m+n)\frac{\partial\hat{U}_n^{(m)}}{\partial\theta} + (\frac{\partial e_{22}}{\partial\theta}+e_{26}\frac{\partial^2}{\partial\theta^2})\hat{U}_n^{(m)} + e_{16}(\lambda_m+n)(\lambda_m+n-1)\hat{V}_n^{(m)} + (\frac{\partial e_{26}}{\partial\theta})(\lambda_m+n)\hat{V}_n^{(m)}$$
$$+ (-e_{26}+\frac{\partial e_{22}}{\partial\theta})\frac{\partial\hat{V}_n^{(m)}}{\partial\theta} + (e_{12}+e_{26})(\lambda_m+n)\frac{\partial\hat{V}_n^{(m)}}{\partial\theta} + (-\frac{\partial e_{26}}{\partial\theta}+e_{22}\frac{\partial^2}{\partial\theta^2})\hat{V}_n^{(m)} + e_{15}(\lambda_m+n)\times(\lambda_m+n-1)\hat{W}_n^{(m)}$$
$$+ (e_{15}+\frac{\partial e_{25}}{\partial\theta})(\lambda_m+n)\hat{W}_n^{(m)} + (\frac{\partial e_{24}}{\partial\theta})\frac{\partial\hat{W}_n^{(m)}}{\partial\theta} + (e_{14}+e_{25})(\lambda_m+n)\frac{\partial\hat{W}_n^{(m)}}{\partial\theta} + e_{24}\frac{\partial^2\hat{W}_n^{(m)}}{\partial\theta^2} - \eta_{11}(\lambda_m+n)(\lambda_m+n-1)\hat{\Phi}_n^{(m)}$$
$$- (\eta_{11}+\frac{\partial\eta_{12}}{\partial\theta})(\lambda_m+n)\hat{\Phi}_n^{(m)} - (\frac{\partial\eta_{22}}{\partial\theta})\frac{\partial\hat{\Phi}_n^{(m)}}{\partial\theta} - 2\eta_{12}(\lambda_m+n)\frac{\partial\hat{\Phi}_n^{(m)}}{\partial\theta} - \eta_{22}\frac{\partial^2\hat{\Phi}_n^{(m)}}{\partial\theta^2}] + r^{\lambda_m+n-1}[(e_{15}+e_{32}+\frac{\partial e_{25}}{\partial\theta})\frac{\partial\hat{U}_n^{(m)}}{\partial z}$$
$$+ (e_{25}+e_{36})\frac{\partial^2\hat{U}_n^{(m)}}{\partial\theta\partial z} + (e_{15}+e_{31})(\lambda_m+n)\frac{\partial\hat{U}_n^{(m)}}{\partial z} + (e_{14}-e_{36}+\frac{\partial e_{24}}{\partial\theta})\frac{\partial\hat{V}_n^{(m)}}{\partial z} + (e_{24}+e_{32})\frac{\partial^2\hat{V}_n^{(m)}}{\partial\theta\partial z}$$
$$+ (e_{14}+e_{36})(\lambda_m+n)\frac{\partial\hat{V}_n^{(m)}}{\partial z} + (e_{13}+\frac{\partial e_{23}}{\partial\theta})\frac{\partial\hat{W}_n^{(m)}}{\partial z} + (e_{13}+e_{35})(\lambda_m+n)\frac{\partial\hat{W}_n^{(m)}}{\partial z} - (\eta_{13}+\frac{\partial\eta_{23}}{\partial\theta})\frac{\partial\hat{\Phi}_n^{(m)}}{\partial z} - 2\eta_{23}\frac{\partial^2\hat{\Phi}_n^{(m)}}{\partial\theta\partial z}$$
$$- 2\eta_{13}(\lambda_m+n)\frac{\partial\hat{\Phi}_n^{(m)}}{\partial z}] + r^{\lambda_m+n}(e_{35}\frac{\partial^2\hat{U}_n^{(m)}}{\partial z^2} + e_{34}\frac{\partial^2\hat{V}_n^{(m)}}{\partial z^2} + e_{33}\frac{\partial^2\hat{W}_n^{(m)}}{\partial z^2} - \eta_{33}\frac{\partial^2\hat{\Phi}_n^{(m)}}{\partial z^2}) = 0. \quad (7d)$$

To investigate the behaviors of the solutions around $r = 0$, only the parts of the solutions with the lowest order of r have to be considered. That is the solution corresponding to $n = 0$ in Eqs. (7). Accordingly, the following equations must be solved.

$$\frac{\partial^2\hat{U}_0^{(m)}}{\partial\theta^2} + p_1(\theta)\frac{\partial\hat{U}_0^{(m)}}{\partial\theta} + p_2(\theta)\hat{U}_0^{(m)} + p_3(\theta)\frac{\partial^2\hat{V}_0^{(m)}}{\partial\theta^2} + p_4(\theta)\frac{\partial\hat{V}_0^{(m)}}{\partial\theta} + p_5(\theta)\hat{V}_0^{(m)} + p_6(\theta)\frac{\partial^2\hat{W}_0^{(m)}}{\partial\theta^2} + p_7(\theta)\frac{\partial\hat{W}_0^{(m)}}{\partial\theta}$$
$$+ p_8(\theta)\hat{W}_0^{(m)} + p_9(\theta)\frac{\partial^2\hat{\Phi}_0^{(m)}}{\partial\theta^2} + p_{10}(\theta)\frac{\partial\hat{\Phi}_0^{(m)}}{\partial\theta} + p_{11}(\theta)\hat{\Phi}_0^{(m)} = 0, \quad (8a)$$

$$\frac{\partial^2\hat{V}_0^{(m)}}{\partial\theta^2} + q_1(\theta)\frac{\partial\hat{V}_0^{(m)}}{\partial\theta} + q_2(\theta)\hat{V}_0^{(m)} + q_3(\theta)\frac{\partial^2\hat{U}_0^{(m)}}{\partial\theta^2} + q_4(\theta)\frac{\partial\hat{U}_0^{(m)}}{\partial\theta} + q_5(\theta)\hat{U}_0^{(m)} + q_6(\theta)\frac{\partial^2\hat{W}_0^{(m)}}{\partial\theta^2} + q_7(\theta)\frac{\partial\hat{W}_0^{(m)}}{\partial\theta}$$
$$+ q_8(\theta)\hat{W}_0^{(m)} + q_9(\theta)\frac{\partial^2\hat{\Phi}_0^{(m)}}{\partial\theta^2} + q_{10}(\theta)\frac{\partial\hat{\Phi}_0^{(m)}}{\partial\theta} + q_{11}(\theta)\hat{\Phi}_0^{(m)} = 0, \quad (8b)$$

$$\frac{\partial^2\hat{W}_0^{(m)}}{\partial\theta^2} + r_1(\theta)\frac{\partial\hat{W}_0^{(m)}}{\partial\theta} + r_2(\theta)\hat{W}_0^{(m)} + r_3(\theta)\frac{\partial^2\hat{U}_0^{(m)}}{\partial\theta^2} + r_4(\theta)\frac{\partial\hat{U}_0^{(m)}}{\partial\theta} + r_5(\theta)\hat{U}_0^{(m)} + r_6(\theta)\frac{\partial^2\hat{V}_0^{(m)}}{\partial\theta^2} + r_7(\theta)\frac{\partial\hat{V}_0^{(m)}}{\partial\theta}$$
$$+ r_8(\theta)\hat{V}_0^{(m)} + r_9(\theta)\frac{\partial^2\hat{\Phi}_0^{(m)}}{\partial\theta^2} + r_{10}(\theta)\frac{\partial\hat{\Phi}_0^{(m)}}{\partial\theta} + r_{11}(\theta)\hat{\Phi}_0^{(m)} = 0, \quad (8c)$$

$$\frac{\partial^2\hat{\Phi}_0^{(m)}}{\partial\theta^2}+s_1(\theta)\frac{\partial\hat{\Phi}_0^{(m)}}{\partial\theta}+s_2(\theta)\hat{\Phi}_0^{(m)}+s_3(\theta)\frac{\partial^2\hat{U}_0^{(m)}}{\partial\theta^2}+s_4(\theta)\frac{\partial\hat{U}_0^{(m)}}{\partial\theta}+s_5(\theta)\hat{U}_0^{(m)}+s_6(\theta)\frac{\partial^2\hat{V}_0^{(m)}}{\partial\theta^2}+s_7(\theta)\frac{\partial\hat{V}_0^{(m)}}{\partial\theta}+s_8(\theta)\hat{V}_0^{(m)}$$
$$+s_9(\theta)\frac{\partial^2\hat{W}_0^{(m)}}{\partial\theta^2}+s_{10}(\theta)\frac{\partial\hat{W}_0^{(m)}}{\partial\theta}+s_{11}(\theta)\hat{W}_0^{(m)}=0. \tag{8d}$$

Appendix III defines p_i, qi, r_i, and s_i in Eqs. (8).

Eqs. (8) are a set of ordinary differential equations with variable coefficients that depend only on θ. The solutions to Eqs. (8) are independent of z. The exact closed-form solutions to Eqs. (8) are intractable, if they exist. The power series method can be directly adopted to develop a general solution for ordinary differential equations with variable coefficients. Very high-order terms must be considered to obtain an accurate solution and this requirement can cause numerical difficulties. To overcome these difficulties, a domain decomposition technique is used in conjunction with the power series method to establish a general solution of Eqs. (8).

The range of θ under consideration is first divided into a number of sub-domains (see Fig. 2). A series solution to Eqs. (8) is established in each sub-domain. Consequently, a general solution over the whole θ domain is constructed from these series solutions in the sub-domains by imposing the continuity conditions between each pair of adjacent sub-domains. This process is a very convenient means of constructing solutions that can be used to analyze multi-material wedges, which are also considered in this work.

To establish the power series solution for sub-domain i of θ, the variable coefficients in Eqs. (8) are expanded in terms of the power series of θ with respect to the middle point of the sub-domain, $\bar{\theta}_i$:

$$p_j(\theta)=\sum_{k=0}^{K}(\mu_j)_k^{(i)}(\theta-\bar{\theta}_i)^k,\quad q_j(\theta)=\sum_{k=0}^{K}(\varsigma_j)_k^{(i)}(\theta-\bar{\theta}_i)^k, r_j(\theta)=\sum_{k=0}^{K}(\xi_j)_k^{(i)}(\theta-\bar{\theta}_i)^k,\quad s_j(\theta)=\sum_{k=0}^{K}(\vartheta_j)_k^{(i)}(\theta-\bar{\theta}_i)^k. \tag{9}$$

Similarly, the solutions of Eqs. (8) in sub-domain i are expressed as,

$$\hat{U}_{0i}^{(m)}=\sum_{j=0}^{J}\hat{A}_j^{(i)}(\theta-\bar{\theta}_i)^j,\hat{V}_{0i}^{(m)}=\sum_{j=0}^{J}\hat{B}_j^{(i)}(\theta-\bar{\theta}_i)^j,\hat{W}_{0i}^{(m)}=\sum_{j=0}^{J}\hat{C}_j^{(i)}(\theta-\bar{\theta}_i)^j,\hat{\Phi}_{0i}^{(m)}=\sum_{j=0}^{J}\hat{D}_j^{(i)}(\theta-\bar{\theta}_i)^j. \tag{10}$$

Substituting Eqs. (9) and (10) into Eqs. (8) and carefully rearranging yields the following relations among the coefficients in Eqs. (10),

$$\hat{A}_{j+2}^{(i)}+(\mu_3)_0^{(i)}\hat{B}_{j+2}^{(i)}+(\mu_6)_0^{(i)}\hat{C}_{j+2}^{(i)}+(\mu_9)_0^{(i)}\hat{D}_{j+2}^{(i)}$$
$$=\frac{-1}{(j+2)(j+1)}\{\sum_{k=0}^{j-1}[(k+2)(k+1)((\mu_3)_{j-k}^{(i)}\hat{B}_{k+2}^{(i)}+(\mu_6)_{j-k}^{(i)}\hat{C}_{k+2}^{(i)}+(\mu_9)_{j-k}^{(i)}\hat{D}_{k+2}^{(i)})]+\sum_{k=0}^{j}[(k+1)(\mu_1)_{j-k}^{(i)}\hat{A}_{k+1}^{(i)}+(\mu_2)_{j-k}^{(i)}\hat{A}_k^{(i)}$$
$$+(k+1)(\mu_4)_{j-k}^{(i)}\hat{B}_{k+1}^{(i)}+(\mu_5)_{j-k}^{(i)}\hat{B}_k^{(i)}+(k+1)(\mu_7)_{j-k}^{(i)}\hat{C}_{k+1}^{(i)}+(\mu_8)_{j-k}^{(i)}\hat{C}_k^{(i)}+(k+1)(\mu_{10})_{j-k}^{(i)}\hat{D}_{k+1}^{(i)}+(\mu_{11})_{j-k}^{(i)}\hat{D}_k^{(i)}]\}, \tag{11a}$$

$$\hat{B}_{j+2}^{(i)}+(\varsigma_3)_0^{(i)}\hat{A}_{j+2}^{(i)}+(\varsigma_6)_0^{(i)}\hat{C}_{j+2}^{(i)}+(\varsigma_9)_0^{(i)}\hat{D}_{j+2}^{(i)}$$
$$=\frac{-1}{(j+2)(j+1)}\{\sum_{k=0}^{j-1}[(k+2)(k+1)((\varsigma_3)_{j-k}^{(i)}\hat{A}_{k+2}^{(i)}+(\varsigma_6)_{j-k}^{(i)}\hat{C}_{k+2}^{(i)}+(\varsigma_9)_{j-k}^{(i)}\hat{D}_{k+2}^{(i)})]+\sum_{k=0}^{j}[(k+1)(\varsigma_1)_{j-k}^{(i)}\hat{B}_{k+1}^{(i)}$$
$$+(\varsigma_2)_{j-k}^{(i)}\hat{B}_k^{(i)}+(k+1)(\varsigma_4)_{j-k}^{(i)}\hat{A}_{k+1}^{(i)}+(\varsigma_5)_{j-k}^{(i)}\hat{A}_k^{(i)}+(k+1)(\varsigma_7)_{j-k}^{(i)}\hat{C}_{k+1}^{(i)}+(\varsigma_8)_{j-k}^{(i)}\hat{C}_k^{(i)}+(k+1)(\varsigma_{10})_{j-k}^{(i)}\hat{D}_{k+1}^{(i)}+(\varsigma_{11})_{j-k}^{(i)}\hat{D}_k^{(i)}]\}, \tag{11b}$$

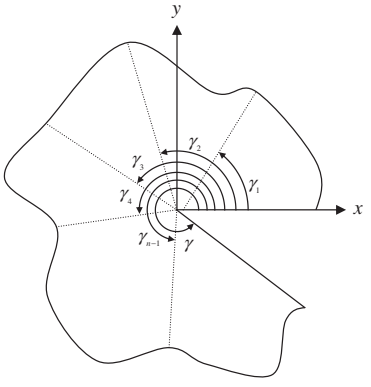

Fig. 2. Sub-domains for $\theta \in [0, \gamma]$.

$$\hat{C}^{(i)}_{j+2}+(\xi_3)^{(i)}_0\hat{A}^{(i)}_{j+2}+(\xi_6)^{(i)}_0\hat{B}^{(i)}_{j+2}+(\xi_9)^{(i)}_0\hat{D}^{(i)}_{j+2}$$
$$=\frac{-1}{(j+2)(j+1)}\{\sum_{k=0}^{j-1}[(k+2)(k+1)((\xi_3)^{(i)}_{j-k}\hat{A}^{(i)}_{k+2}+(\xi_6)^{(i)}_{j-k}\hat{B}^{(i)}_{k+2}+(\xi_9)^{(i)}_{j-k}\hat{D}^{(i)}_{k+2})]+\sum_{k=0}^{j}[(k+1)(\xi_1)^{(i)}_{j-k}\hat{C}^{(i)}_{k+1}+(\xi_2)^{(i)}_{j-k}\hat{C}^{(i)}_{k}$$
$$+(k+1)(\xi_4)^{(i)}_{j-k}\hat{A}^{(i)}_{k+1}+(\xi_5)^{(i)}_{j-k}\hat{A}^{(i)}_{k}+(k+1)(\xi_7)^{(i)}_{j-k}\hat{B}^{(i)}_{k+1}+(\xi_8)^{(i)}_{j-k}\hat{B}^{(i)}_{k}+(k+1)(\xi_{10})^{(i)}_{j-k}\hat{D}^{(i)}_{k+1}+(\xi_{11})^{(i)}_{j-k}\hat{D}^{(i)}_{k}]\},\tag{11c}$$

$$\hat{D}^{(i)}_{j+2}+(\vartheta_3)^{(i)}_0\hat{A}^{(i)}_{j+2}+(\vartheta_6)^{(i)}_0\hat{B}^{(i)}_{j+2}+(\vartheta_9)^{(i)}_0\hat{C}^{(i)}_{j+2}$$
$$=\frac{-1}{(j+2)(j+1)}\{\sum_{k=0}^{j-1}[(k+2)(k+1)((\vartheta_3)^{(i)}_{j-k}\hat{A}^{(i)}_{k+2}+(\vartheta_6)^{(i)}_{j-k}\hat{B}^{(i)}_{k+2}+(\vartheta_9)^{(i)}_{j-k}\hat{C}^{(i)}_{k+2})]+\sum_{k=0}^{j}[(k+1)(\vartheta_1)^{(i)}_{j-k}\hat{D}^{(i)}_{k+1}+(\vartheta_2)^{(i)}_{j-k}\hat{D}^{(i)}_{k}$$
$$+(k+1)(\vartheta_4)^{(i)}_{j-k}\hat{A}^{(i)}_{k+1}+(\vartheta_5)^{(i)}_{j-k}\hat{A}^{(i)}_{k}+(k+1)(\vartheta_7)^{(i)}_{j-k}\hat{B}^{(i)}_{k+1}+(\vartheta_8)^{(i)}_{j-k}\hat{B}^{(i)}_{k}+(k+1)(\vartheta_{10})^{(i)}_{j-k}\hat{C}^{(i)}_{k+1}+(\vartheta_{11})^{(i)}_{j-k}\hat{C}^{(i)}_{k+1}]\}.\tag{11d}$$

Close examination of Eqs. (11) reveals that if $\hat{A}^{(i)}_0$, $\hat{A}^{(i)}_1$, $\hat{B}^{(i)}_0$, $\hat{B}^{(i)}_1$, $\hat{C}^{(i)}_0$, $\hat{C}^{(i)}_1$, $\hat{D}^{(i)}_0$ and $\hat{D}^{(i)}_1$ are determined, then the other coefficients in Eqs. (10) ($\hat{A}^{(i)}_j$, $\hat{B}^{(i)}_j$, $\hat{C}^{(i)}_j$ and $\hat{D}^{(i)}_j$, $j\geqslant 2$) can be found by solving the linear algebraic equations in Eqs. (11). Consequently, the solutions to Eqs. (8) in sub-domain i of θ can be expressed as

$$\hat{U}^{(m)}_{0i}(\theta,z)=\hat{A}^{(i)}_0\hat{U}^{(m)}_{0i0}(\theta)+\hat{A}^{(i)}_1\hat{U}^{(m)}_{0i1}(\theta)+\hat{B}^{(i)}_0\hat{U}^{(m)}_{0i2}(\theta)+\hat{B}^{(i)}_1\hat{U}^{(m)}_{0i3}(\theta)+\hat{C}^{(i)}_0\hat{U}^{(m)}_{0i4}(\theta)+\hat{C}^{(i)}_1\hat{U}^{(m)}_{0i5}(\theta)+\hat{D}^{(i)}_0\hat{U}^{(m)}_{0i6}(\theta)+\hat{D}^{(i)}_1\hat{U}^{(m)}_{0i7}(\theta),\tag{12a}$$

$$\hat{V}^{(m)}_{0i}(\theta,z)=\hat{A}^{(i)}_0\hat{V}^{(m)}_{0i0}(\theta)+\hat{A}^{(i)}_1\hat{V}^{(m)}_{0i1}(\theta)+\hat{B}^{(i)}_0\hat{V}^{(m)}_{0i2}(\theta)+\hat{B}^{(i)}_1\hat{V}^{(m)}_{0i3}(\theta)+\hat{C}^{(i)}_0\hat{V}^{(m)}_{0i4}(\theta)+\hat{C}^{(i)}_1\hat{V}^{(m)}_{0i5}(\theta)+\hat{D}^{(i)}_0\hat{V}^{(m)}_{0i6}(\theta)+\hat{D}^{(i)}_1\hat{V}^{(m)}_{0i7}(\theta),\tag{12b}$$

$$\hat{W}^{(m)}_{0i}(\theta,z)=\hat{A}^{(i)}_0\hat{W}^{(m)}_{0i0}(\theta)+\hat{A}^{(i)}_1\hat{W}^{(m)}_{0i1}(\theta)+\hat{B}^{(i)}_0\hat{W}^{(m)}_{0i2}(\theta)+\hat{B}^{(i)}_1\hat{W}^{(m)}_{0i3}(\theta)+\hat{C}^{(i)}_0\hat{W}^{(m)}_{0i4}(\theta)+\hat{C}^{(i)}_1\hat{W}^{(m)}_{0i5}(\theta)+\hat{D}^{(i)}_0\hat{W}^{(m)}_{0i6}(\theta)+\hat{D}^{(i)}_1\hat{W}^{(m)}_{0i7}(\theta),\tag{12c}$$

$$\hat{\Phi}^{(m)}_{0i}(\theta,z)=\hat{A}^{(i)}_0\hat{\Phi}^{(m)}_{0i0}(\theta)+\hat{A}^{(i)}_1\hat{\Phi}^{(m)}_{0i1}(\theta)+\hat{B}^{(i)}_0\hat{\Phi}^{(m)}_{0i2}(\theta)+\hat{B}^{(i)}_1\hat{\Phi}^{(m)}_{0i3}(\theta)+\hat{C}^{(i)}_0\hat{\Phi}^{(m)}_{0i4}(\theta)+\hat{C}^{(i)}_1\hat{\Phi}^{(m)}_{0i5}(\theta)+\hat{D}^{(i)}_0\hat{\Phi}^{(m)}_{0i6}(\theta)+\hat{D}^{(i)}_1\hat{\Phi}^{(m)}_{0i7}(\theta).\tag{12d}$$

The asymptotic solution in sub-domain i of θ is,

$$u^{(i)}_r(r,\theta,z)=\sum_{m=0}^{\infty}r^{\lambda_m}\hat{U}^{(m)}_{0i}(\theta,z)+O(r^{\lambda_m+1})=\tilde{u}^{(i)}_r(r,\theta,z,\lambda_m)+O(r^{\lambda_m+1}),\tag{13a}$$

$$u^{(i)}_\theta(r,\theta,z)=\sum_{m=0}^{\infty}r^{\lambda_m}\hat{V}^{(m)}_{0i}(\theta,z)+O(r^{\lambda_m+1})=\tilde{u}^{(i)}_\theta(r,\theta,z,\lambda_m)+O(r^{\lambda_m+1}),\tag{13b}$$

$$u^{(i)}_z(r,\theta,z)=\sum_{m=0}^{\infty}r^{\lambda_m}\hat{W}^{(m)}_{0i}(\theta,z)+O(r^{\lambda_m+1})=\tilde{u}^{(i)}_z(r,\theta,z,\lambda_m)+O(r^{\lambda_m+1}),\tag{13c}$$

$$\phi^{(i)}(r,\theta,z)=\sum_{m=0}^{\infty}r^{\lambda_m}\hat{\Phi}^{(m)}_{0i}(\theta,z)+O(r^{\lambda_m+1})=\tilde{\phi}^{(i)}(r,\theta,z,\lambda_m)+O(r^{\lambda_m+1}).\tag{13d}$$

When the range of θ is decomposed into n sub-domains, a total of $8n$ coefficients must be determined in all of the sub-domain solutions that are constructed using the above procedure. These solutions must satisfy the continuity conditions between pairs of adjacent sub-domains. These include continuities of tractions, mechanical displacements, electric displacements and electric potential. These continuity conditions yield $8(n-1)$ algebraic equations. Homogenous boundary conditions at $\theta=\theta_0$ and $\theta=\theta_n$ must be satisfied, yielding another eight equations. As a result, $8n$ coefficients are to be determined from $8n$ homogenous algebraic equations. A nontrivial solution for the coefficients yields an $8n\times 8n$ matrix with a determinant of zero. The roots of the zero determinant (λ_m), which can be complex numbers, are obtained herein using the numerical approach of Müller [34].

4. Verification of solution

To validate the proposed solution, convergence studies for minimum Re[λ_m] (real part of λ_m) are conducted by increasing the number of sub-domains or increasing the number of polynomial terms in each sub-domain, and the convergent solutions are compared with the published results. The wedges under consideration are made of piezoelectric material PZT-4, which is transversely isotropic. Table 1 presents the material properties of PZT-4.

Table 1
Material properties.

Material	Stiffness [GPa]					Piezoelectric const. [C/m^2]			Dielectric const. $\times 10^{-10}$ [F/m]	
	$\hat{c}_{11}$	$\hat{c}_{12}$	$\hat{c}_{13}$	$\hat{c}_{33}$	$\hat{c}_{44}$	$\hat{e}_{15}$	$\hat{e}_{31}$	$\hat{e}_{33}$	$\hat{\eta}_{11}$	$\hat{\eta}_{33}$
PZT-4	139.0	77.8	74.3	115.0	25.6	12.7	-5.2	15.1	64.6	56.2
PZT-5H	126.0	55.0	53.0	117.0	35.3	17.0	-6.5	23.3	151.0	130.0
Si	166.2	64.6	64.6	166.2	50.8	–	–	–	–	–

Table 2
Convergence of minimum Re[λ_m] for PZT-4 wedges.

γ	Boundary conditions	Number of sub-domains	Terms									Published results
			5	6	7	8	9	10	12	14	15	
360°	FOFO	3	0.4985	0.4978	0.4916	0.4417	0.4980	0.4998	0.4750	0.5000	0.4999	0.5000 [29]
		4	0.4996	0.4963	0.4993	0.4999	0.4999	0.4984	0.4999	0.4999	0.4999	
		6	0.5000	0.4993	0.4999	0.4999	0.5000	0.5000	0.4999	0.5000	0.5000	
		8	0.4999	0.4999	0.4999	0.4999	0.4999	0.5000	0.5000	0.4999	0.5000	
360°	FOCC	3	0.1769	0.1969	0.2052	0.1602	0.1718	0.1965	0.1724	0.1954	0.1895	0.1869 [18]
		4	0.1855	0.1895	0.1847	0.1877	0.1879	0.1857	0.1877	0.1865	0.1869	
		6	0.1869	0.1869	0.1869	0.1869	0.1869	0.1869	0.1869	0.1869	0.1869	
		8	0.1869	0.1869	0.1869	0.1869	0.1869	0.1869	0.1869	0.1869	0.1869	
180°		2	0.3710	0.3751	0.3749	0.3740	0.3736	0.3735	0.3741	0.3737	0.3738	0.3739 [18]
		3	0.3741	0.3737	0.3738	0.3739	0.3739	0.3739	0.3739	0.3739	0.3737	
		4	0.3738	0.3739	0.3739	0.3739	0.3739	0.3739	0.3739	0.3739	0.3739	
		6	0.3739	0.3739	0.3739	0.3739	0.3739	0.3739	0.3739	0.3739	0.3739	

Table 3
Comparisons between the present and the published λ_m for PZT-4 wedges.

γ	Boundary conditions	Direction of polarization	Roots of λ_m	Published results	Present results
360°	FOCC	Y	λ_0	0.1869[a]	0.1869
			λ_1	0.3131[a]	0.3131
			λ_2	0.6869[a]	0.6869
357°	FOFO	Y	λ_0	0.5000[b]	0.5000
			λ_1	0.5094[b]	0.5094
			λ_2	0.5046[b]	0.5046
		Z	λ_0	0.5000[b]	0.5000
			λ_1	0.5085[b]	0.5085
			λ_2	0.5042[b]	0.5042
330°	FOFO	Y	λ_0	0.5021[b]	0.5021
			λ_1	0.5499[b]	0.5498
			λ_2	0.6109[b]	0.6109
		Z	λ_0	0.5015[b]	0.5014
			λ_1	0.5455[b]	0.5455
			λ_2	0.5982[b]	0.5981
180°	FOCC	Y	λ_0	0.3739[a]	0.3739
			λ_1	0.5000[a]	0.5000
			λ_2	0.6261[a]	0.6261

Note:
[a] Denotes the results of Hwu and Ikeda [18].
[b] Denotes the results of Sze et al. [24].

Table 2 considers three cases. Four letters specify the boundary conditions of a wedge at $\theta = 0$ and $\theta = \gamma$. The first and third letters represent the mechanical boundary conditions at $\theta = 0$ and $\theta = \gamma$, respectively; and C and F represent clamped and free boundary conditions, respectively. Similarly, the second and fourth letters concern the electric boundary conditions with C and O's denoting electrically closed and open boundary conditions, respectively. These rules are adopted throughout the paper.

The first case concerns a crack problem with a material having its direction of polarization in the z direction (see Fig. 1). The surfaces of the crack are free of surface traction and surface charge. That is $\sigma_{\theta\theta} = \sigma_{\theta r} = \sigma_{\theta z} = D_\theta = 0$ at $\theta = 0$ and 2π. The results of Sosa and Pak [29] were obtained by using an eigenfunction approach, which is similar to the present approach. Sosa and Pak [29] examined a piezoelectric parallelepiped with a cut-through crack and having its direction of polarization in the z direction, so that they could find a closed-form solution for λ_m.

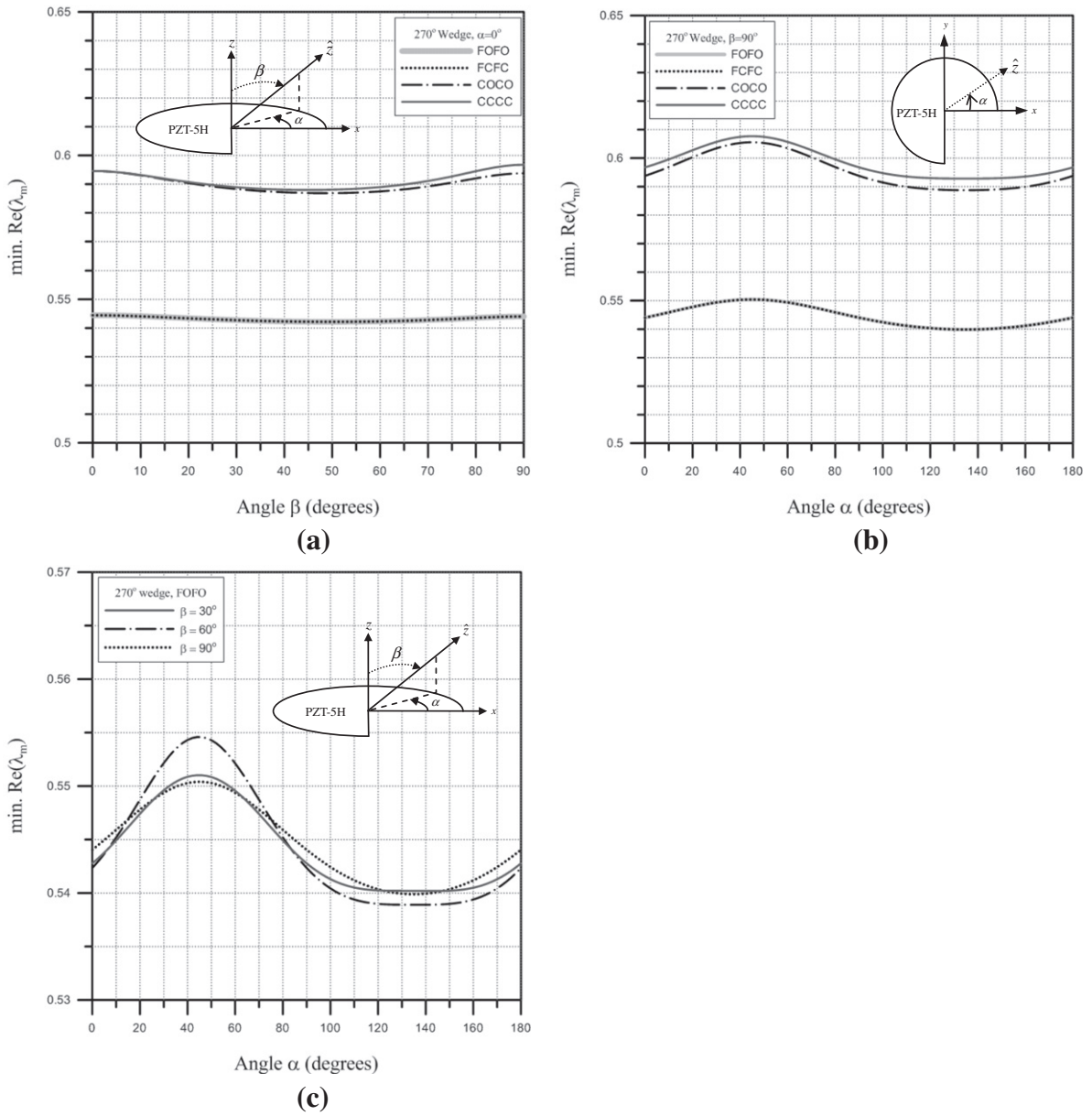

Fig. 3. Variation of minimum Re[λ_m] with direction of polarization for a 270° PZT-5H wedge (a) $\alpha = 0°$ (on x–z plane), (b) $\beta = 90°$ (on x–y plane), (c) $\beta = 30°$, 60° and 90°.

The other two cases involve 180° and 360° wedges with FOCC boundary conditions and polarization along $\theta = 180°$ and $\theta = 270°$, respectively, in the plane x–y. Table 2 also presents the results that were published by Hwu and Ikeda [18]. Notably, the solutions of Hwu and Ikeda [18] are two-dimensional solutions, depending on x and y, and are based on the assumption of generalized plane strain and a short circuit. They assumed $\varepsilon_{zz} = 0$ and $E_z = 0$, eliminated the terms that were associated with ε_{zz} and E_z in the constitutive equations, and replaced σ_{zz} and D_z by the other stress and electric displacement components. Thus, they eliminated c_{ij} (i or $j = 3$), e_{k6} and η_{k3} from Eqs. (4). Using their assumptions and following the present solution procedure shown in Sections 2 and 3, one can obtain exactly the same equations as Eqs. (8) and the same values of λ_m given in the present work. This fact is indirectly evidenced by two observations. The first is that the terms corresponding to the derivatives with respect to z in Eqs. (5) are absent from Eqs. (8), indicating that the assumption of all physical quantities in Eqs. (5) independent of z does not affect the establishment of Eqs. (8). The other is that the coefficients in Eqs. (8), presented in Appendix III, are independence of c_{ij}(i or $j = 3$), e_{k6} and η_{k3}.

The comparison in Table 2 of the convergent values obtained herein with those published reveals excellent agreement. The present convergent solutions can be obtained by increasing the number of sub-domains or increasing the order of

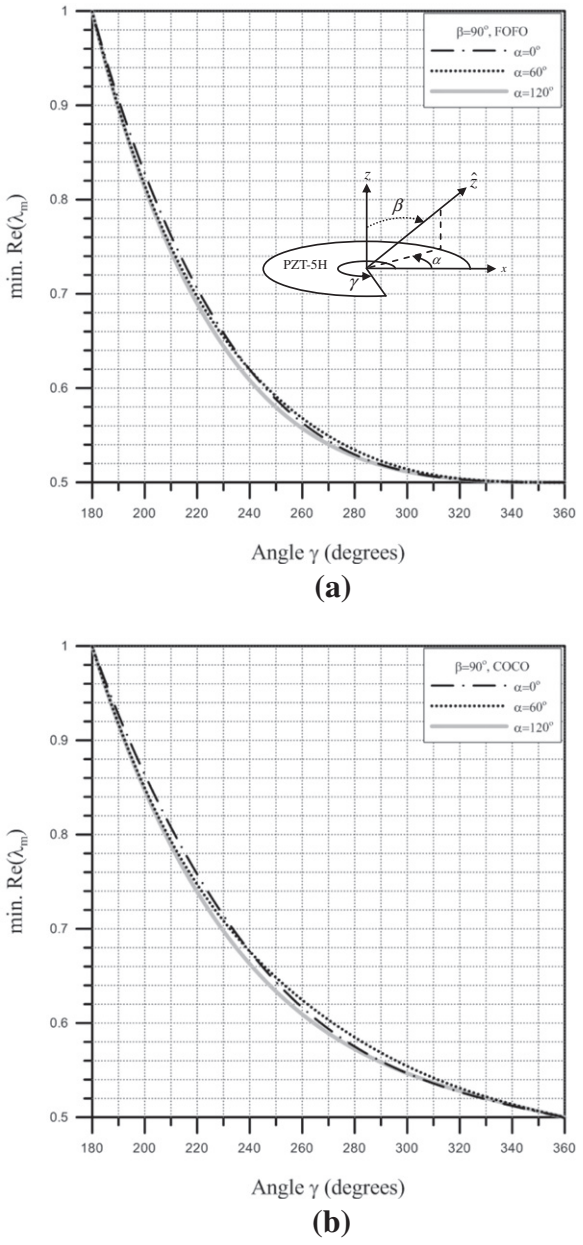

Fig. 4. Variation of minimum Re[λ_m] with wedge angle for PZT-5H wedges (a) FOFO boundary conditions, (b) COCO boundary conditions.

the polynomials. Using a large number of sub-domains in combination with a small number of polynomial terms can yield convergent results without any numerical difficulty.

It is also interesting to demonstrate the accuracy of the values of λ_m other than minimum Re[λ_m] obtained by the present approach. Herein, λ_m are in order of Re[λ_i] $\leqslant$ Re[λ_{i+1}] (i = 0, 1, 2,...). Table 3 compares λ_0, λ_1 and λ_2 determined by the present approach with the results published by Hwu and Ikeda [18] and Sze and Wang [24] for PZT-4 wedges with different γ, boundary conditions and directions of polarization. Notably, the results of Sze and Wang [24] were obtained by a finite element approach with three-dimensional formulations and assuming all the physical quantities under consideration independent on z. The material properties of PZT-4, which were used in Sze and Wang [24] and are different from those given in Table 3, were applied for the wedges with FOFO boundary conditions in Table 3. The different material properties from those in Table 1 and used in Sze and Wang [24] are $\hat{c}_{33}$ = 113 GPa, $\hat{e}_{15}$ = 13.44 C/m^2, $\hat{e}_{31}$ = −6.98 C/m^2, $\hat{e}_{33}$ = 13.84 C/m^2, $\hat{\eta}_{11} = 60.0 \times 10^{-10}$ F/m, and $\hat{\eta}_{33} = 54.7 \times 10^{-10}$ F/m. The present results were obtained by dividing the whole domain of θ into four sub-domains and using 12 polynomial terms in the solutions for each sub-domain. Table 3 discloses excellent agreement between the present and the published results.

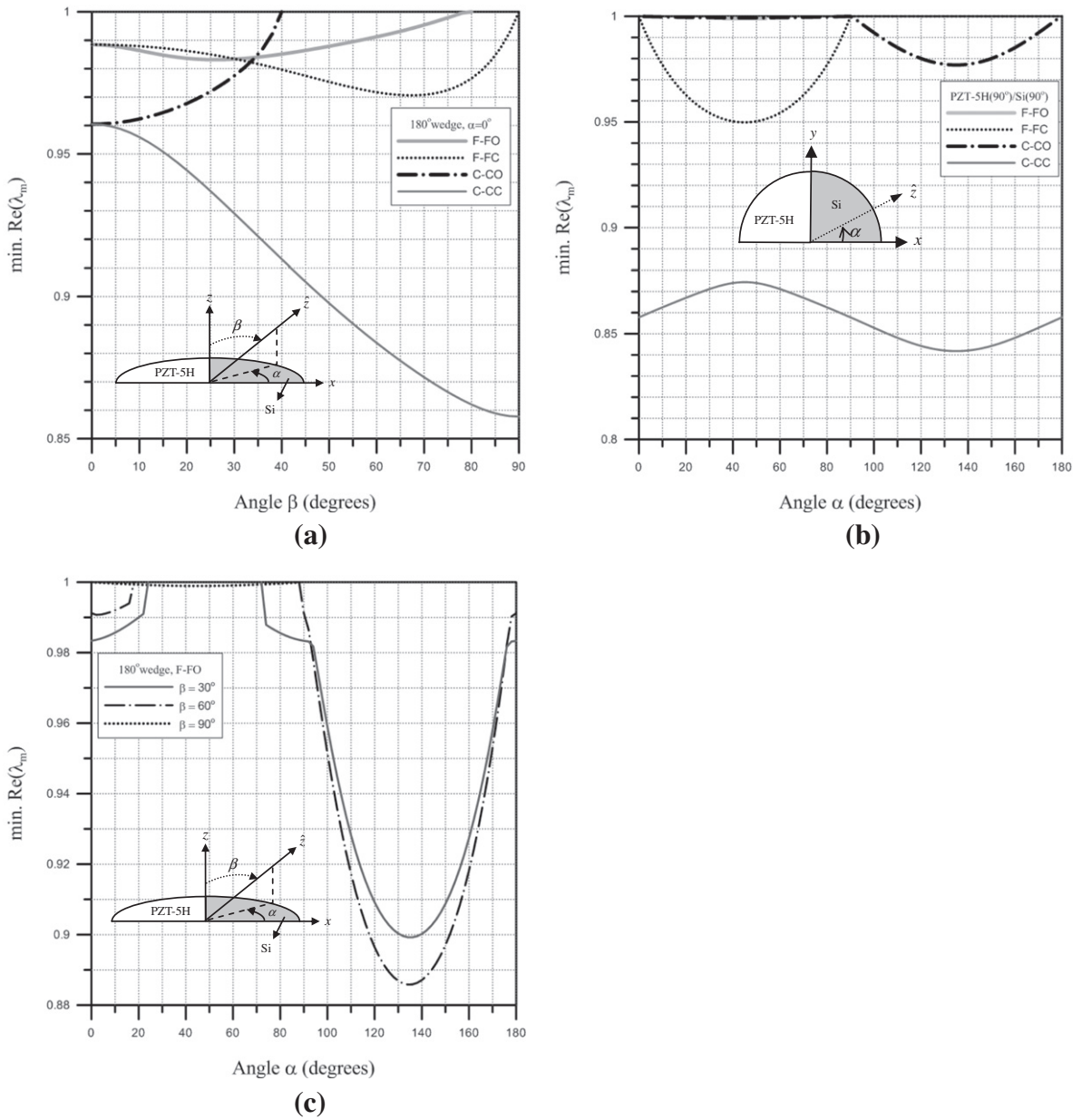

Fig. 5. Variation of minimum Re[λ_m] with direction of polarization for a 180° PZT-5H/Si bi-material wedge (a) $\alpha = 0°$ (on x–z plane), (b) $\beta = 90°$ (on x–y plane), (c) $\beta = 30°$, 60° and 90°.

5. Numerical results and discussion

After the correctness of the proposed solutions was verified by performing the convergence studies and comparisons with the published results, the proposed solution was further applied to investigate the electroelastic singularities in a piezoelectric wedge with varying directions of polarization. The wedges under consideration are made of a single piezoelectric material, a piezoelectric material and an isotropic elastic material, or two piezoelectric materials. Two parameters α and β are introduced to specify the direction of polarization, where α is the angle between the x-axis and the projection of the polarization axis onto the x–y plane, and β is the angle between the z axis and the polarization axis. The order of electroelastic singularity at the apex of a wedge is determined by the real part of $(\lambda_m - 1)$, and the root of primary interest is the one with the smallest positive real part between zero and one. The following presents the values of minimum Re[λ_m] for wedges with various combinations of boundary conditions along $\theta = 0$ and $\theta = \gamma$.

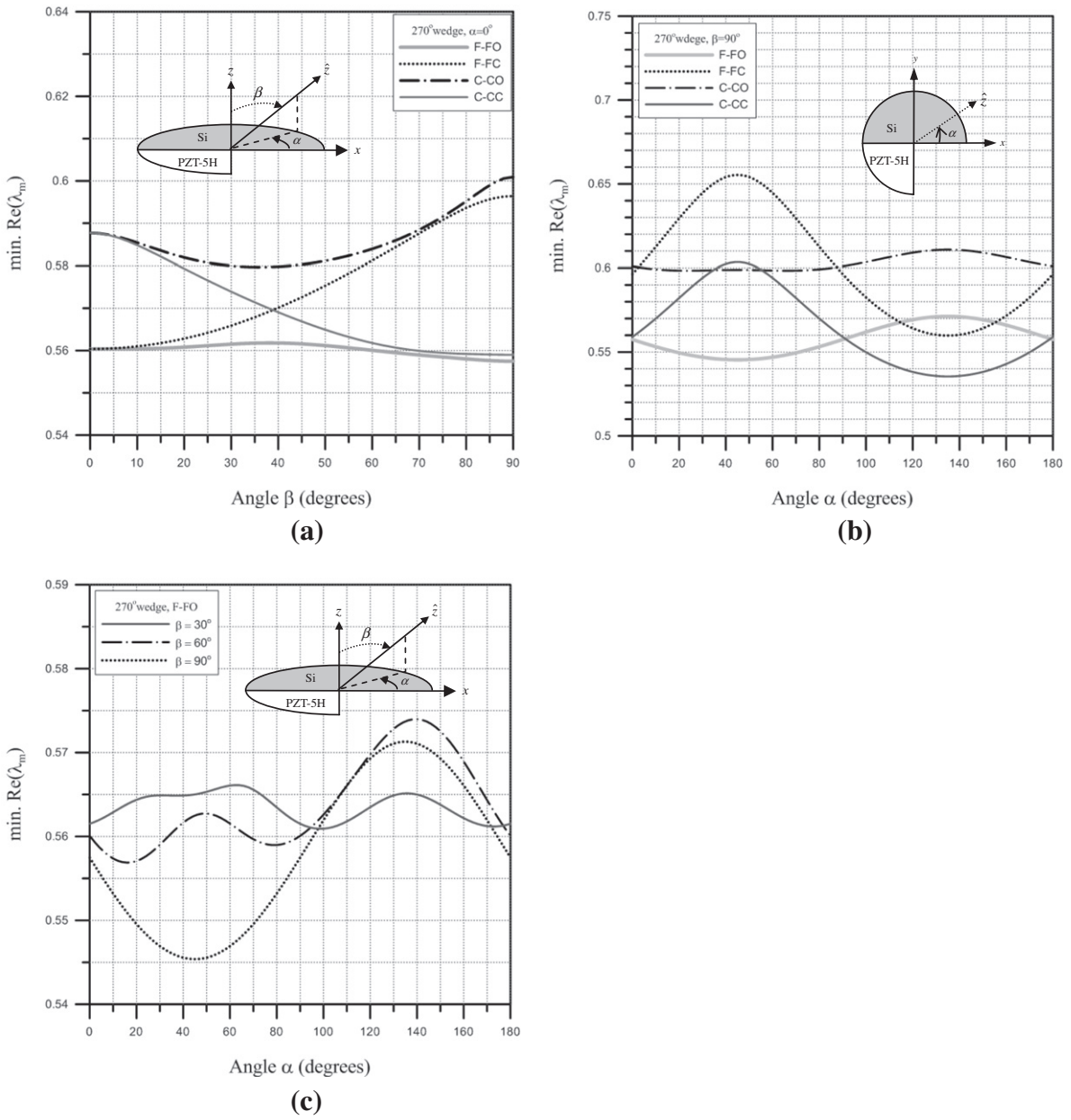

Fig. 6. Variation of minimum Re[λ_m] with direction of polarization for a 270° PZT-5H/Si bi-material wedge (a) $\alpha = 0°$ (on x–z plane), (b) $\beta = 90°$ (on x–y plane), (c) $\beta = 30°$, 60° and 90°.

5.1. Wedges made of a single piezoelectric material

Figure 3 illustrates the effects of the direction of polarization on the minimum values of Re[λ_m] for a 270° wedge made of PZT-5H, whose material properties are given in Table 1. Four combinations of boundary conditions were considered – FOFO, FCFC, COCO and CCCC. As stated in Section 4, FOFO means free mechanical boundary conditions and open electric boundary conditions at both of $\theta = 0°$ and $\theta = 270°$. In Fig. 3a, $\alpha = 0°$ means that the direction of polarization is in the x–z plane, while $\beta = 90°$ in Fig. 3b indicates that the direction of polarization is in the x–y plane. Figure 3a only considers $0^o \leqslant \beta \leqslant 90^o$ because β+90° and 90°$-\beta$ yield the same λ_m. Similarly, Fig. 3b only presents the results for $0^o \leqslant \alpha \leqslant 180^o$ because α+180° and 180°$-\alpha$ have the same λ_m. Figure 3a and b demonstrate that the FF mechanical boundary conditions cause more severe electroelastic singularities than do the CC mechanical boundary conditions. Electric boundary conditions do not affect minimum Re[λ_m] in the FCFC and FOFO cases. The variation in minimum Re[λ_m] owing to changes in the direction of polarization is less than 5%.

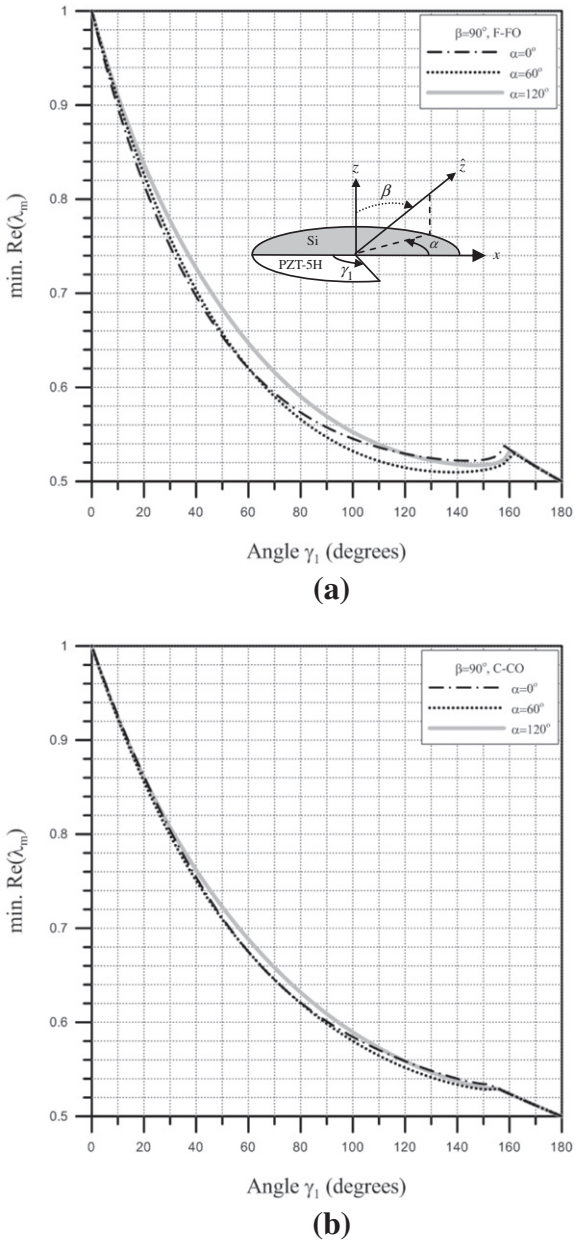

Fig. 7. Variation of minimum Re[λ_m] with wedge angle for PZT-5H/Si wedges (a) F-FO boundary conditions, (b) C-CO boundary conditions.

Figure 4 plots the variation of minimum Re[λ_m] of PZT-5H wedges with wedge angle γ and under FOFO and COCO boundary conditions. Three different directions of polarization in the x–y plane were considered – $\alpha = 0°$, 60°, and 120°. The λ_m values that correspond to minimum Re[λ_m] are all real. As expected, minimum Re[λ_m] decreases as γ increases; and the FOFO boundary conditions yield a smaller minimum Re[λ_m] than do the COCO boundary conditions. When $\gamma = 360°$ (representing a crack), both sets of boundary conditions result in $\lambda_m = 0.5$, and the orientation of the polarization in the x–y plane does not influence the singularity order.

5.2. Bi-material wedges made of piezoelectric and elastic materials

The integration of piezoelectric films on silicon (Si) substrates is favored in the design and formation of micro electromechanical systems. This section study the electroelastic singularities at the interface in wedges that are made of PZT-5H and Si, whose material properties are found in Table 1. Two typical wedge configurations – those of 180° and 270° wedges – were

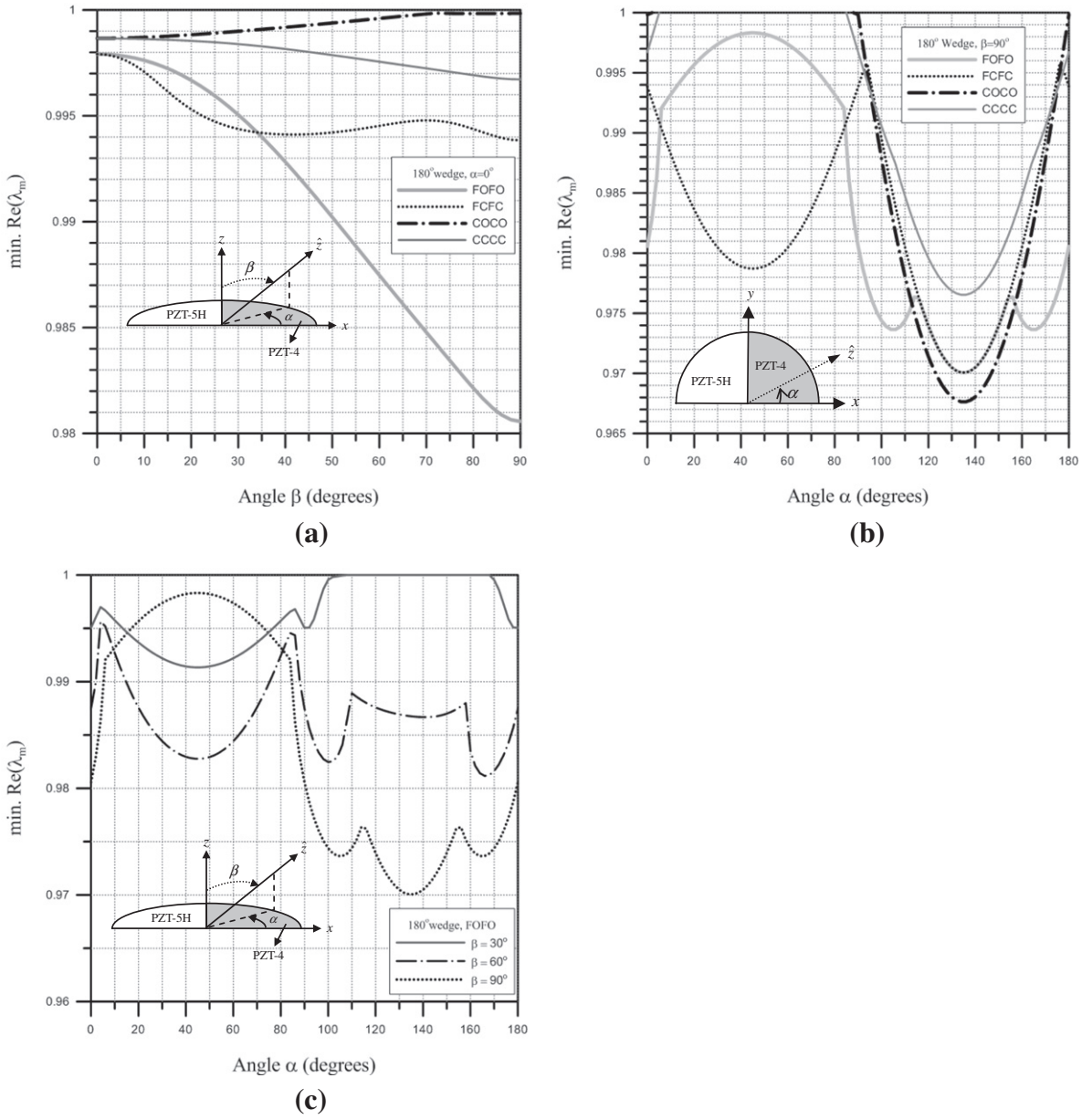

Fig. 8. Variation of minimum Re[λ_m] with direction of polarization for a 180° PZT-5H/ PZT-4 bi-material wedge (a) $\alpha = 0°$ (on x–z plane), (b) $\beta = 90°$ (on x–y plane), (c) $\beta = 30°$, 60° and 90°.

considered first. In a 180° wedge, Si and PZT-5H occupy $0^{\circ} \leqslant \theta \leqslant 90^{\circ}$ and $90^{\circ} \leqslant \theta \leqslant 180^{\circ}$, respectively, while in a 270° wedge, Si and PZT-5H occupy $0^{\circ} \leqslant \theta \leqslant 180^{\circ}$ and $180^{\circ} \leqslant \theta \leqslant 270^{\circ}$, respectively. Figure 5 an 6 plot the values of minimum Re[λ_m] of these two wedges versus their directions of polarization, respectively. Again, four sets of boundary conditions were considered. These are F-FO, F-FC, C-CO, and C-CC, where "-" denotes the absence of any electric boundary conditions at $\theta = 0°$, according to the rule for defining boundary conditions described in Section 4.

In Fig. 5a and b, the directions of polarization of PZT-5H are in the x–z plane and x–y plane, respectively, while Fig. 5c displays the results for the wedges with the F-FO boundary conditions and having the directions of polarization on the surfaces with $\beta = 30°$, 60° and 90°. It is interesting to observe that the direction of polarization can be especially arranged to eliminate electroelastic singularities at the interface of the wedge. For example, Fig. 5a reveals no electroelastic singularities when $80^{\circ} \leqslant \beta \leqslant 90^{\circ}$ and $38^{\circ} \leqslant \beta \leqslant 90^{\circ}$ for boundary conditions F-FO and C-CO, respectively; Fig. 5b shows no electroelastic singularities when $90^{\circ} < \alpha \leqslant 180^{\circ}$ under boundary conditions F-FO and F-FC, and Fig. 5c shows no electroelastic

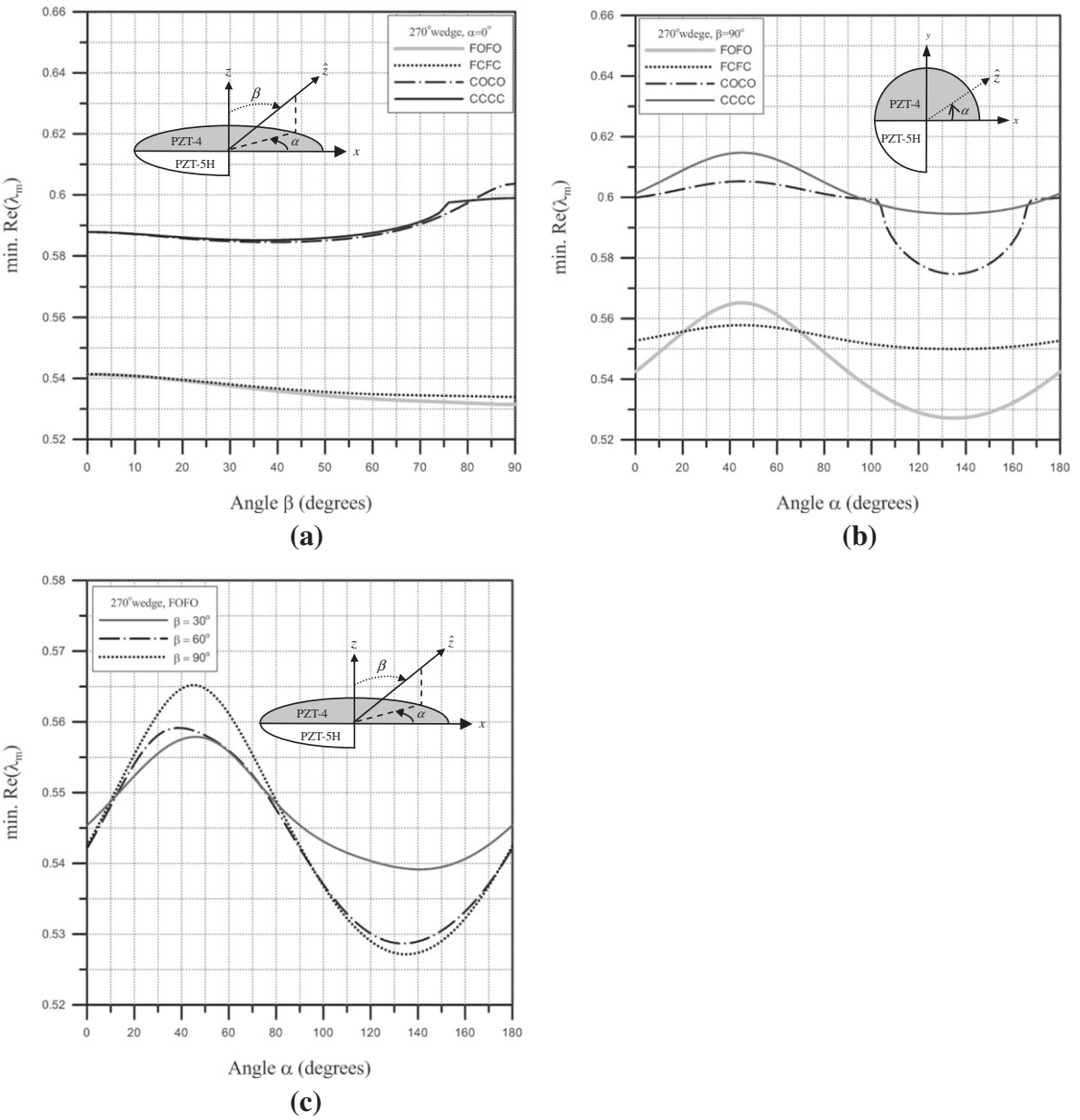

Fig. 9. Variation of minimum Re[λ_m] with direction of polarization for a 270° PZT-5H/PZT-4 bi-material wedge (a) $\alpha = 0°$ (on x–z plane), (b) $\beta = 90°$ (on x–y plane), (c) $\beta = 30°$, 60° and 90°.

singularities when $18° < \alpha < 88°$ and $23° < \alpha < 72°$ under the conditions $\beta = 60°$ and 30°, respectively. Notably, boundary conditions C-CC yield more severe singularities at the interface than do the other three sets of boundary conditions.

According to Fig. 6, in investigating the singularities in 270° wedges, changes in the direction of polarization may yield considerable changes in minimum Re[λ_m]. In Fig. 6a, the order of the singularity falls by approximately 10% under boundary conditions F-FO as β changes from 0° to 90°, and in Fig. 6b, it increases by about 25% under boundary conditions F-FC as α changes from 45° to 135° .

Figure 7a and b plot the variation of minimum Re[λ_m] with the angle of PZT-5H, γ_1, under boundary conditions F-FO and C-CO, respectively. In the wedges in Fig. 7, Si occupies $0^\circ \leqslant \theta \leqslant 180^\circ$, and the wedge angle γ equals $\gamma_1 + 180°$. The directions of polarization are in the x–y plane and $\alpha = 0°$, 60° and 120°. As expected, the strength of the singularity generally increases with the increase of γ_1, and the order of the singularity equals 0.5 when $\gamma_1 = 180°$ (representing a crack). The relatively abrupt changes of the minimum Re[λ_m] around $\gamma_1 = 160°$ in Fig. 7a are caused by the changes of λ_m from real numbers to complex numbers.

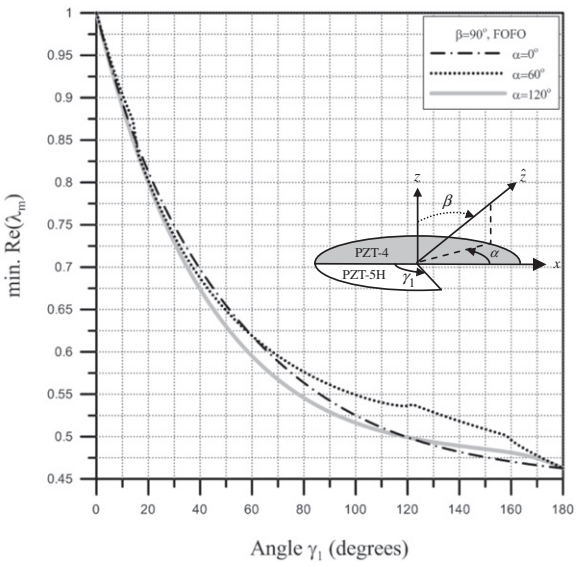

Fig. 10. Variation of minimum Re[λ_m] with wedge angle for PZT-5H/PZT-4 wedges (a) FOFO boundary conditions, (b) COCO boundary conditions.

5.3. Bi-material wedges made of piezoelectric materials

Bi-material wedges that comprise piezoelectric materials are commonly encountered in smart structures. This section investigates electroelastic singularities at the interface of bi-material wedges comprised of PZT-5H and PZT-4, whose material properties are provided in Table 1. The configurations of wedges considered in this section are the same as those in the preceding section, except in that the elastic material in the previous section is replaced by the piezoelectric material PZT-4.

Figure 8 illustrate the effects of the orientations of polarization on the electroelastic singularities in wedges with a wedge angle 180°. When the direction of polarization lies in the x–y plane (see Fig. 8b), $2° < \alpha < 88°$ and $6° < \alpha < 84°$ yield no singularities under boundary conditions COCO and CCCC, respectively. When the direction of polarization is on the surface with $\beta = 30°$ (see Fig. 8c), no singularities are found for $108° < \alpha < 168°$ under the FOFO boundary conditions. Changes in the direction of polarization alter the order of the singularity by less than 4%.

Free–free mechanical boundary conditions cause more severe electroelastic singularities in 270° wedges (Fig. 9) than do clamped–clamped boundary conditions. The orientation of polarization may change the order of the singularity by approximately 9%. For wedges with other angles, that percentage exceeds 10% (Fig. 10).

6. Concluding remarks

This study found an asymptotic solution to a piezoelectric wedge to investigate geometrically-induced electroelastic singularities at the vertex of the wedge based on three-dimensional piezoelasticity theory in a cylindrical coordinate system. The piezoelectric material is first assumed to be anisotropic and its direction of polarization to be arbitrary. The solution was obtained using an eigenfunction expansion approach in conjunction with a power series technique to solve the equilibrium and Maxwell's equations, which are four coupled partial differential equations in terms of the displacement components and electric potential. The present solution is easily reduced to the solution for anisotropic elastic wedges by eliminating the piezoelastic and dielectric constants. The proposed solution is verified by performing convergence studies and comparing the results with the published results.

The proposed solution was employed to examine electroelastic singularities in wedges that comprise a single piezoelectric material (PZT-5H), bounded piezo/isotropic elastic materials (PZT-5H/Si), or piezo/piezo materials (PZT-5H/PZT-4). The minimum Re[λ_m], which is directly related to the order of the singularity, is displayed for different wedge angles, combinations of boundary conditions, and directions of polarization. As expected, the strength of the singularity generally increases with the increase of wedge angle. Interestingly, the direction of polarization can be set to eliminate the singularities at the interface of 180°wedges made of PZT-5H/Si or PZT-5H/PZT-4 with free-free mechanical boundary conditions. This phenomenon is particularly important because such wedges are frequently encountered in many smart structures.

Acknowledgements

This work reported herein was supported by the National Science Council, Taiwan through research Grant No. NSC100-2221-E-009-093-MY2. This support is gratefully acknowledged.

Appendix I

$$[c] = [\mathrm{T}]_\sigma [\mathrm{K}][\hat{c}][\mathrm{K}]^{\mathrm{T}}[\mathrm{T}]_\varepsilon^{-1}, [e] = [\mathrm{T}]_{\mathrm{D}}[\mathrm{L}][\hat{e}][\mathrm{K}]^{\mathrm{T}}[\mathrm{T}]_\varepsilon^{-1}, [\eta] = [\mathrm{T}]_{\mathrm{D}}[\mathrm{L}][\hat{\eta}][\mathrm{L}]^{\mathrm{T}}[\mathrm{T}]_{\mathrm{E}}^{-1}$$

where

$$[\mathrm{T}]_\sigma = \begin{bmatrix} \cos^2\theta & \sin^2\theta & 0 & 0 & 0 & 2\cos\theta\sin\theta \\ \sin^2\theta & \cos^2\theta & 0 & 0 & 0 & -2\cos\theta\sin\theta \\ 0 & 0 & 1 & 0 & 0 & 0 \\ 0 & 0 & 0 & \cos\theta & -\sin\theta & 0 \\ 0 & 0 & 0 & \sin\theta & \cos\theta & 0 \\ -\cos\theta\sin\theta & \cos\theta\sin\theta & 0 & 0 & 0 & \cos^2\theta - \sin^2\theta \end{bmatrix},$$

$$[\mathbf{T}]_\varepsilon = \begin{bmatrix} \cos^2\theta & \sin^2\theta & 0 & 0 & 0 & \cos\theta\sin\theta \\ \sin^2\theta & \cos^2\theta & 0 & 0 & 0 & -\cos\theta\sin\theta \\ 0 & 0 & 1 & 0 & 0 & 0 \\ 0 & 0 & 0 & \cos\theta & -\sin\theta & 0 \\ 0 & 0 & 0 & \sin\theta & \cos\theta & 0 \\ -2\cos\theta\sin\theta & 2\cos\theta\sin\theta & 0 & 0 & 0 & \cos^2\theta - \sin^2\theta \end{bmatrix},$$

$$[\mathrm{T}]_E = [\mathrm{T}]_D = \begin{bmatrix} \cos\theta & \sin\theta & 0 \\ -\sin\theta & \cos\theta & 0 \\ 0 & 0 & 1 \end{bmatrix},$$

$$[\mathrm{L}] = \begin{bmatrix} \cos(x,\hat{x}) & \cos(x,\hat{y}) & \cos(x,\hat{z}) \\ \cos(y,\hat{x}) & \cos(y,\hat{y}) & \cos(y,\hat{z}) \\ \cos(z,\hat{x}) & \cos(z,\hat{y}) & \cos(z,\hat{z}) \end{bmatrix} = \begin{bmatrix} l_{11} & l_{12} & l_{13} \\ l_{21} & l_{22} & l_{23} \\ l_{31} & l_{32} & l_{33} \end{bmatrix},$$

$$[\mathrm{K}] = \begin{bmatrix} \mathrm{K}_1 & 2K_2 \\ \mathrm{K}_3 & \mathrm{K}_4 \end{bmatrix},$$

$$K_1 = \begin{bmatrix} l_{11}^2 & l_{12}^2 & l_{13}^2 \\ l_{21}^2 & l_{22}^2 & l_{23}^2 \\ l_{31}^2 & l_{32}^2 & l_{33}^2 \end{bmatrix}, K_2 = \begin{bmatrix} l_{12}l_{13} & l_{13}l_{11} & l_{11}l_{12} \\ l_{22}l_{23} & l_{23}l_{21} & l_{21}l_{22} \\ l_{32}l_{33} & l_{33}l_{31} & l_{31}l_{32} \end{bmatrix}, K_3 = \begin{bmatrix} l_{21}l_{31} & l_{22}l_{32} & l_{23}l_{33} \\ l_{31}l_{11} & l_{32}l_{12} & l_{33}l_{13} \\ l_{11}l_{21} & l_{12}l_{22} & l_{13}l_{23} \end{bmatrix},$$

$$K_4 = \begin{bmatrix} l_{22}l_{33} + l_{23}l_{32} & l_{23}l_{31} + l_{21}l_{33} & l_{21}l_{32} + l_{22}l_{31} \\ l_{32}l_{13} + l_{33}l_{12} & l_{33}l_{11} + l_{31}l_{13} & l_{31}l_{12} + l_{32}l_{11} \\ l_{12}l_{23} + l_{13}l_{22} & l_{13}l_{21} + l_{11}l_{23} & l_{11}l_{22} + l_{12}l_{21} \end{bmatrix}$$

Appendix II

$$\sigma_{rr} = c_{11}\frac{\partial u_r}{\partial r} + c_{12}\left(\frac{1}{r}\frac{\partial u_\theta}{\partial \theta} + \frac{u_r}{r}\right) + c_{13}\frac{\partial u_z}{\partial z} + c_{14}\left(\frac{\partial u_\theta}{\partial z} + \frac{1}{r}\frac{\partial u_z}{\partial \theta}\right) + c_{15}\left(\frac{\partial u_z}{\partial r} + \frac{\partial u_r}{\partial z}\right)$$

$$+c_{16}\left(\frac{1}{r}\frac{\partial u_r}{\partial \theta} + \frac{\partial u_\theta}{\partial r} - \frac{u_\theta}{r}\right) + e_{11}\frac{\partial \phi}{\partial r} + e_{21}\frac{1}{r}\frac{\partial \phi}{\partial \theta} + e_{31}\frac{\partial \phi}{\partial z}$$

$$\sigma_{zz} = c_{13}\frac{\partial u_r}{\partial r} + c_{23}\left(\frac{1}{r}\frac{\partial u_\theta}{\partial \theta} + \frac{u_r}{r}\right) + c_{33}\frac{\partial u_z}{\partial z} + c_{34}\left(\frac{\partial u_\theta}{\partial z} + \frac{1}{r}\frac{\partial u_z}{\partial \theta}\right) + c_{35}\left(\frac{\partial u_z}{\partial r} + \frac{\partial u_r}{\partial z}\right)$$

$$+c_{36}\left(\frac{1}{r}\frac{\partial u_r}{\partial \theta} + \frac{\partial u_\theta}{\partial r} - \frac{u_\theta}{r}\right) + e_{13}\frac{\partial \phi}{\partial r} + e_{23}\frac{1}{r}\frac{\partial \phi}{\partial \theta} + e_{33}\frac{\partial \phi}{\partial z}$$

$$\sigma_{z\theta} = c_{14}\frac{\partial u_r}{\partial r} + c_{24}\left(\frac{1}{r}\frac{\partial u_\theta}{\partial \theta} + \frac{u_r}{r}\right) + c_{34}\frac{\partial u_z}{\partial z} + c_{44}\left(\frac{\partial u_\theta}{\partial z} + \frac{1}{r}\frac{\partial u_z}{\partial \theta}\right) + c_{45}\left(\frac{\partial u_z}{\partial r} + \frac{\partial u_r}{\partial z}\right)$$

$$+c_{46}\left(\frac{1}{r}\frac{\partial u_r}{\partial \theta} + \frac{\partial u_\theta}{\partial r} - \frac{u_\theta}{r}\right) + e_{14}\frac{\partial \phi}{\partial r} + e_{24}\frac{1}{r}\frac{\partial \phi}{\partial \theta} + e_{34}\frac{\partial \phi}{\partial z}$$

$$\sigma_{\theta\theta} = c_{12}\frac{\partial u_r}{\partial r} + c_{22}\left(\frac{1}{r}\frac{\partial u_\theta}{\partial \theta} + \frac{u_r}{r}\right) + c_{23}\frac{\partial u_z}{\partial z} + c_{24}\left(\frac{\partial u_\theta}{\partial z} + \frac{1}{r}\frac{\partial u_z}{\partial \theta}\right) + c_{25}\left(\frac{\partial u_z}{\partial r} + \frac{\partial u_r}{\partial z}\right)$$

$$+c_{26}\left(\frac{1}{r}\frac{\partial u_r}{\partial \theta} + \frac{\partial u_\theta}{\partial r} - \frac{u_\theta}{r}\right) + e_{12}\frac{\partial \phi}{\partial r} + e_{22}\frac{1}{r}\frac{\partial \phi}{\partial \theta} + e_{32}\frac{\partial \phi}{\partial z}$$

$$\sigma_{zr} = c_{15}\frac{\partial u_r}{\partial r} + c_{25}\left(\frac{1}{r}\frac{\partial u_\theta}{\partial \theta} + \frac{u_r}{r}\right) + c_{35}\frac{\partial u_z}{\partial z} + c_{45}\left(\frac{\partial u_\theta}{\partial z} + \frac{1}{r}\frac{\partial u_z}{\partial \theta}\right) + c_{55}\left(\frac{\partial u_z}{\partial r} + \frac{\partial u_r}{\partial z}\right)$$

$$+c_{56}\left(\frac{1}{r}\frac{\partial u_r}{\partial \theta} + \frac{\partial u_\theta}{\partial r} - \frac{u_\theta}{r}\right) + e_{15}\frac{\partial \phi}{\partial r} + e_{25}\frac{1}{r}\frac{\partial \phi}{\partial \theta} + e_{35}\frac{\partial \phi}{\partial z}$$

$$\sigma_{r\theta} = c_{16}\frac{\partial u_r}{\partial r} + c_{26}\left(\frac{1}{r}\frac{\partial u_\theta}{\partial \theta} + \frac{u_r}{r}\right) + c_{36}\frac{\partial u_z}{\partial z} + c_{46}\left(\frac{\partial u_\theta}{\partial z} + \frac{1}{r}\frac{\partial u_z}{\partial \theta}\right) + c_{56}\left(\frac{\partial u_z}{\partial r} + \frac{\partial u_r}{\partial z}\right)$$

$$+c_{66}\left(\frac{1}{r}\frac{\partial u_r}{\partial \theta} + \frac{\partial u_\theta}{\partial r} - \frac{u_\theta}{r}\right) + e_{16}\frac{\partial \phi}{\partial r} + e_{26}\frac{1}{r}\frac{\partial \phi}{\partial \theta} + e_{36}\frac{\partial \phi}{\partial z}$$

$$D_r = e_{11}\frac{\partial u_r}{\partial r} + e_{12}\left(\frac{1}{r}\frac{\partial u_\theta}{\partial \theta} + \frac{u_r}{r}\right) + e_{13}\frac{\partial u_z}{\partial z} + e_{14}\left(\frac{\partial u_\theta}{\partial z} + \frac{1}{r}\frac{\partial u_z}{\partial \theta}\right) + e_{15}\left(\frac{\partial u_z}{\partial r} + \frac{\partial u_r}{\partial z}\right)$$

$$+e_{16}\left(\frac{1}{r}\frac{\partial u_r}{\partial \theta} + \frac{\partial u_\theta}{\partial r} - \frac{u_\theta}{r}\right) - \eta_{11}\frac{\partial \phi}{\partial r} - \eta_{12}\frac{1}{r}\frac{\partial \phi}{\partial \theta} - \eta_{13}\frac{\partial \phi}{\partial z}$$

$$D_\theta = e_{21}\frac{\partial u_r}{\partial r} + e_{22}\left(\frac{1}{r}\frac{\partial u_\theta}{\partial \theta} + \frac{u_r}{r}\right) + e_{23}\frac{\partial u_z}{\partial z} + e_{24}\left(\frac{\partial u_\theta}{\partial z} + \frac{1}{r}\frac{\partial u_z}{\partial \theta}\right) + e_{25}\left(\frac{\partial u_z}{\partial r} + \frac{\partial u_r}{\partial z}\right)$$

$$+e_{26}\left(\frac{1}{r}\frac{\partial u_r}{\partial \theta} + \frac{\partial u_\theta}{\partial r} - \frac{u_\theta}{r}\right) - \eta_{12}\frac{\partial \phi}{\partial r} - \eta_{22}\frac{1}{r}\frac{\partial \phi}{\partial \theta} - \eta_{23}\frac{\partial \phi}{\partial z}$$

$$D_z = e_{31}\frac{\partial u_r}{\partial r} + e_{32}\left(\frac{1}{r}\frac{\partial u_\theta}{\partial \theta} + \frac{u_r}{r}\right) + e_{33}\frac{\partial u_z}{\partial z} + e_{34}\left(\frac{\partial u_\theta}{\partial z} + \frac{1}{r}\frac{\partial u_z}{\partial \theta}\right) + e_{35}\left(\frac{\partial u_z}{\partial r} + \frac{\partial u_r}{\partial z}\right)$$

$$+e_{36}\left(\frac{1}{r}\frac{\partial u_r}{\partial \theta} + \frac{\partial u_\theta}{\partial r} - \frac{u_\theta}{r}\right) - \eta_{13}\frac{\partial \phi}{\partial r} - \eta_{23}\frac{1}{r}\frac{\partial \phi}{\partial \theta} - \eta_{33}\frac{\partial \phi}{\partial z}$$

where the electric potential, φ, is related to the electric field by,

$$E_r = \frac{\partial \phi}{\partial r}, E_\theta = \frac{1}{r}\frac{\partial \phi}{\partial \theta} \quad \text{and} \quad E_z = \frac{\partial \phi}{\partial z}.$$

Appendix III

$$p_1(\theta) = \frac{1}{c_{66}}\left(2\lambda_m c_{16} + \frac{\partial c_{66}}{\partial \theta}\right), p_2(\theta) = \frac{1}{c_{66}}\left(\lambda_m^2 c_{11} + \lambda_m \frac{\partial c_{16}}{\partial \theta} - c_{22} + \frac{\partial c_{26}}{\partial \theta}\right), p_3(\theta) = \frac{c_{26}}{c_{66}},$$

$$p_4(\theta) = \frac{1}{c_{66}}\left[(\lambda_m - 1)c_{66} + \lambda_m c_{12} - c_{22} + \frac{\partial c_{26}}{\partial \theta}\right], p_5(\theta) = \frac{1}{c_{66}}(\lambda_m - 1)\left(\lambda_m c_{16} - c_{26} + \frac{\partial c_{66}}{\partial \theta}\right), p_6(\theta) = \frac{c_{46}}{c_{66}},$$

$$p_7(\theta) = \frac{1}{c_{66}}\left[\lambda_m(c_{14} + c_{56}) - c_{24} + \frac{\partial c_{46}}{\partial \theta}\right], p_8(\theta) = \frac{1}{c_{66}}\lambda_m\left(\lambda_m c_{15} - c_{25} + \frac{\partial c_{56}}{\partial \theta}\right), p_9(\theta) = \frac{e_{26}}{c_{66}},$$

$$p_{10}(\theta) = \frac{1}{c_{66}}\left[\lambda_m(e_{16} + e_{21}) - e_{22} + \frac{\partial e_{26}}{\partial \theta}\right], p_{11}(\theta) = \frac{1}{c_{66}}\lambda_m\left(\lambda_m e_{11} - e_{12} + \frac{\partial e_{16}}{\partial \theta}\right)$$

$$q_1(\theta) = \frac{1}{c_{22}}\left(2\lambda_m c_{26} + \frac{\partial c_{22}}{\partial \theta}\right), q_2(\theta) = \frac{1}{c_{22}}(\lambda_m - 1)\left[(\lambda_m + 1)c_{66} + \frac{\partial c_{26}}{\partial \theta}\right], q_3(\theta) = \frac{c_{26}}{c_{22}},$$

$$q_4(\theta) = \frac{1}{c_{22}}\left[\lambda_m(c_{12} + c_{66}) + c_{66} + c_{22} + \frac{\partial c_{26}}{\partial \theta}\right], q_5(\theta) = \frac{1}{c_{22}}\left[(\lambda_m + 1)(\lambda_m c_{16} + c_{26}) + \lambda_m \frac{\partial c_{12}}{\partial \theta} + \frac{\partial c_{22}}{\partial \theta}\right],$$

$$q_6(\theta) = \frac{c_{24}}{c_{22}}, q_7(\theta) = \frac{1}{c_{22}}\left[\lambda_m(c_{25} + c_{46}) + c_{46} + \frac{\partial c_{24}}{\partial \theta}\right], q_8(\theta) = \lambda_m\left[(\lambda_m + 1)c_{56} + \frac{\partial c_{25}}{\partial \theta}\right],$$

$$q_9(\theta) = \frac{e_{22}}{c_{22}}, q_{10}(\theta) = \frac{1}{c_{22}}\left[\lambda_m(e_{12} + e_{26}) + e_{26} + \frac{\partial e_{22}}{\partial \theta}\right], q_{11}(\theta) = \frac{1}{c_{22}}\lambda_m\left[(\lambda_m + 1)e_{16} + \frac{\partial e_{12}}{\partial \theta}\right]$$

$$r_1(\theta) = \frac{1}{c_{44}}(2\lambda_m c_{45} + \frac{\partial c_{44}}{\partial \theta}), r_2(\theta) = \frac{1}{c_{44}}\lambda_m\left(\lambda_m c_{55} + \frac{\partial c_{45}}{\partial \theta}\right), r_3(\theta) = \frac{c_{46}}{c_{44}},$$

$$r_4(\theta) = \frac{1}{c_{44}}\left[\lambda_m(c_{14} + c_{56}) + c_{24} + \frac{\partial c_{46}}{\partial \theta}\right], r_5(\theta) = \frac{1}{c_{44}}\left[\lambda_m\left(\lambda_m c_{15} + c_{25} + \frac{\partial c_{14}}{\partial \theta}\right) + \frac{\partial c_{24}}{\partial \theta}\right], r_6(\theta) = \frac{c_{24}}{c_{44}},$$

$$r_7(\theta) = \frac{1}{c_{44}}\left[\lambda_m(c_{25} + c_{46}) - c_{46} + \frac{\partial c_{24}}{\partial \theta}\right], r_8(\theta) = \frac{1}{c_{44}}(\lambda_m - 1)\left(\lambda_m c_{56} + \frac{\partial c_{46}}{\partial \theta}\right), r_9(\theta) = \frac{e_{24}}{c_{44}},$$

$$r_{10}(\theta) = \frac{1}{c_{44}}\left[\lambda_m(e_{14} + e_{25}) + \frac{\partial e_{24}}{\partial \theta}\right], r_{11}(\theta) = \frac{1}{c_{44}}\lambda_m\left(\lambda_m e_{15} + \frac{\partial e_{14}}{\partial \theta}\right)$$

$$s_1(\theta) = \frac{1}{\eta_{22}}\left(2\lambda_m \eta_{12} + \frac{\partial \eta_{22}}{\partial \theta}\right), s_2(\theta) = \frac{1}{\eta_{22}}\lambda_m\left(\lambda_m \eta_{11} + \frac{\partial \eta_{12}}{\partial \theta}\right), s_3(\theta) = -\frac{e_{26}}{\eta_{22}},$$

$$s_4(\theta) = -\frac{1}{\eta_{22}}\left[\lambda_m(e_{16}+e_{21})+e_{22}+\frac{\partial e_{26}}{\partial\theta}\right], s_5(\theta) = -\frac{1}{\eta_{22}}\left[\lambda_m(\lambda_m e_{11}+e_{12}+\frac{\partial e_{21}}{\partial\theta})+\frac{\partial e_{22}}{\partial\theta}\right],$$

$$s_6(\theta) = -\frac{e_{22}}{\eta_{22}}, s_7(\theta) = -\frac{1}{\eta_{22}}\left[\lambda_m(e_{12}+e_{26})-e_{26}+\frac{\partial e_{22}}{\partial\theta}\right], s_8(\theta) = -\frac{1}{\eta_{22}}(\lambda_m-1)\left(\lambda_m e_{16}+\frac{\partial e_{26}}{\partial\theta}\right),$$

$$s_9(\theta) = -\frac{e_{24}}{\eta_{22}}, s_{10}(\theta) = -\frac{1}{\eta_{22}}\left[\lambda_m(e_{14}+e_{25})+\frac{\partial e_{24}}{\partial\theta}\right], s_{11}(\theta) = -\frac{1}{\eta_{22}}\lambda_m\left(\lambda_m e_{15}+\frac{\partial e_{25}}{\partial\theta}\right)$$

References

[1] M.L. William, Stress singularities resulting from various boundary conditions in angular corners of plates in extension, J. Appl. Mech. 19 (1952) 526–528.
[2] M.L. William, Stress singularities resulting from various boundary conditions in angular corners of plates under bending, Proceeding of 1st U.S. National Congress of Applied Mechanics, (1952) 325–329.
[3] V.L. Hein, F. Erdogan, Stress singularities in a two-material wedge, Int. J. Fract. Mech. 7 (1971) 317–330.
[4] J.P. Dempsey, G.B. Sinclair, On the stress singularities in the plate elasticity of the composite wedge, J. Elast. 9 (1979) 373–391.
[5] T.C.T. Ting, S.C. Chou, Edge singularities in anisotropic composites, Int. J. Solids Struct. 17 (1981) 1057–1068.
[6] R.J. Hartranft, G.C. Sih, The use of eigenfunction expansions in the general solution of three-dimensional crack problems, J. Math. Mech. 19 (1969) 123–138.
[7] M. Xie, R.A. Chaudhuri, Three-dimensional stress singularity at a bimaterial interface crack front, Compos. Struct. 40 (1998) 137–147.
[8] A.K. Rao, Stress concentrations and singularities at interfaces corners, Z. Angew. Math. Mech. 51 (1971) 395–406.
[9] I.O. Ojikutu, R.O. Low, R.A. Scott, Stress singularities in laminated composite wedge, Int. J. Solids Struct. 20 (1984) 777–790.
[10] C.S. Huang, M.J. Chang, Corner stress singularities in a FGM thin plate, Int. J. Solids Struct. 44 (2007) 2802–2819.
[11] W.S. Burton, G.B. Sinclair, On the singularities in Reissner's theory for the bending of elastic plates, J. Appl. Mech. 53 (1986) 220–222.
[12] C.S. Huang, Stress singularities at angular corners in first-order shear deformation plate theory, Int. J. Mech. Sci. 45 (2001) 1–20.
[13] O.G. McGee, J.W. Kim, A.W. Leissa, Sharp corners in Mindlin plate vibrations, ASME J. Appl. Mech. 72 (2005) 1–9.
[14] C.S. Huang, On the singularity induced by boundary conditions in a third-order thick plate theory, ASME J. Appl. Mech. 69 (2002) 800–810.
[15] C.S. Huang, Corner stress singularities in a high-order plate theory, Comput. Struct. 82 (2004) 1657–1669.
[16] X.L. Xu, R.K.N.D. Rajapakse, On singularities in composite piezoelectric wedges and junctions, Int. J. Solids Struct. 37 (2000) 3235–3275.
[17] C.H. Chue, C.D. Chen, Decoupled formulation of piezoelectric elasticity under generalized plane deformation and its application to wedge problems, Int. J. Solids Struct. 39 (2002) 3131–3158.
[18] C. Hwu, T. Ikeda, Eletromechanical fracture analysis for corners and cracks in piezoelectric materials, Int. J. Solids Struct. 45 (2008) 5744–5764.
[19] T.H. Chen, C.H. Chue, H.T. Lee, Stress singularities near the apex of a cylindrically polarized piezoelectric wedge, Arch. App. Mech. 74 (2004) 248–261.
[20] C.H. Chue, C.D. Chen, Antiplane stress singularities in a bonded bimaterial piezoelectric wedge, Arch. Appl. Mech. 72 (2003) 673–685.
[21] F. Shang, T. Kitamura, On stress singularity at the interface edge between piezoelectric thin film and elastic substrate, Microsyst. Technol. 11 (2005) 1115–1120.
[22] Z. Wang, B. Zheng, The general solution of three dimensional problems in piezoelectric media, Int. J. Solids Struct. 32 (1995) 105–115.
[23] F. Shang, T. Kitamura, H. Hirakata, I. Kanno, H.M. Kotera, K. Terada, Experimental and theoretical investigations of delamination at free edge of interface between piezoelectric thin films on a substrate, Int. J. Solids Struct. 42 (2005) 1729–1741.
[24] K.Y. Sze, H.T. Wang, H. Fan, A finite element approach for computing edge singularities in piezoelectric materials, Int. J. Solids Struct. 38 (2001) 9233–9252.
[25] M. Scherzer, M. Kuna, Combined analytical and numerical solution of 2D interface corner configurations between dissimilar piezoelectric materials, Int. J. Fract. 127 (2004) 61–99.
[26] M.C. Chen, J.J. Zhu, K.Y. Sze, Electroelastic singularities in piezoelectric-elastic wedges and junctions, Eng. Fract. Mech. 73 (2006) 855–868.
[27] M.C. Chen, X.C. Ping, Finite element analysis of piezoelectric corner configurations and cracks accounting for different electrical permeabilities, Eng. Fract. Mech. 74 (2007) 1511–1524.
[28] M.C. Chen, X.C. Ping, A novel hybrid element analysis for piezoelectric-parent material wedges, Comput. Mech. 40 (2007) 13–24.
[29] H.A. Sosa, Y.E. Pak, Three-dimensional eigenfunction analysis of a crack in a piezoelectric material, Int. J. Solids Struct. 26 (1990) 1–15.
[30] M.C. Chen, Application of finite-part integrals to the three-dimensional fracture problems for piezoelectric media, Part I: Hypersingular integral equation and theoretical analysis, Int. J. Fract. 121 (2003) 133–148.
[31] M.C. Chen, Application of finite-part integrals to the three-dimensional fracture problems for piezoelectric media, Part II: Numerical analysis, Int. J. Fract. 121 (2003) 149–161.
[32] Z.G. Zhou, Z.T. Chen, A 3-D rectangular permeable crack or two 3-D rectangular permeable cracks in a piezoelectric material, Arch. Appl. Mech. 81 (2011) 641–668.
[33] D. Haojiang, C. Weiqiu, Three Dimensional Problems of Piezoelasticity, Nova Science Publishers Inc., New York, 2001.
[34] D.E. Müller, A method for solving algebraic equations using an automatic computer, Math. Tables Aids Comput. 10 (1956) 208–215.